Boundary characteristic orthogonal polynomials method in the vibration analysis of multi-span plates acting upon a moving mass

Hooman Kashani Rad, Mansour Ghalehnovi [*], Hashem Shariatmadar

Dept. of Civil Engineering, Faculty of Engineering, Ferdowsi University of Mashhad, Mashhad, Iran

ABSTRACT

The Boundary Characteristic Orthogonal Polynomials (BCOP) method is used in this study in order to analyze multi-span plates traversed by a moving inertia load traveling on an arbitrary path with constant velocity. The plate is assumed to be free from any support at the longitudinal edges and the spans are made by simply supported constraints at width, i.e. SFSF. The plate's mode shapes are generated by the BCOP method while the boundary condition is satisfied over all computational modes. A free vibration analysis is done in order to find natural frequency. The governing differential equations of motion are derived by Hamilton's principle and the solution in the time domain is found by using the Matrix Exponential method after modeling the problem in state space. All of the convective inertia terms are included in the acceleration derivatives and the responses are presented both for the load moving on the plate's surface ignoring/including the mass inertia effect. A comprehensive parametric study on the plate's mid-spans is carried out for the single, two- and three-span plates, investigating Dynamic Amplification Factor (DAF) versus non-dimensional velocity (V). The effect of mass and aspect ratio along with the location of reference point of calculation on the dynamic behavior of a multi-span plate is investigated and many graphs are generated as spectra. One can easily find the critical velocity as well as the peak deflection for each case study by introducing a corrective factor. The solution under moving mass excitation is obtained by the factor if the same response for moving load is known.

1. Introduction

Dynamic analysis of structures under moving load excitation has been one of the most important challenges for engineers during the last few years. The vast application of this type of loading in many fields of industry has intensified the importance of evaluating the dynamic response of vibrant structures under moving loads. A comprehensive exploration of vibration of structures under concentrated and distributed moving loads has been presented by Fryba (1999) [1] including formulation of motion for most types of structures such as single and multi-span beams, single-span plates and shells. Railroad tracks and bridges, highway bridges, deck of ships, carrying aircrafts and overhead travelling cranes are just some practical examples of real world structures that undergo moving load excitation. Ouyang [2] also has mentioned several engineering application problems in the field of structural dynamics under moving loads. Beams are often the first common structural elements for modeling bridge decks in vibration analysis of such structures due to the simplicity of its governing equations. Along improvements in mathematical and numerical methods in the dynamic analysis area, many researchers use the plate element in their problem modeling since it can reflect the dynamic behavior of vibrating decks more accurately and realistically. Moreover, considering multi-span beams in the analysis can cause more complexities in the equations of motion and analytical solutions encounter major limitations specifically in mode shape generation. Therefore, one can find numerical methods to be more efficient by simply surveying the past literature. A multi-span plate actually seems to be a more appropriate choice for reflecting the dynamic behavior of multi-span bridges. Given the increasing magnitude and velocity of moving loads and vehicles on bridge decks and foundation of structures, many researchers have performed experiments to show the importance of the effects of inertia of moving loads on the dynamic behavior of these structures. For example, an Euler-Bernoulli beam was investigated by Akin et al. [3]. The study investigated a beam acted upon a moving mass for various boundary conditions utilizing the discrete element method. The results of this research study stress the importance of the role of inertia on moving loads, especially for high velocities. The main simplifications considered in that study is ignoring all convective terms of acceleration except for the vertical ones. In another study performed by Esmailzaeh et al. [4], a simply

---

supported Euler-Bernoulli beam was analyzed under uniform partially distributed moving load, where the importance of load inertia and the length of load moving on the beam were recognized as two parameters that had a great effect on the dynamic response of beam. Lee [5] assessed a Timoshenko beam with simply supported boundary conditions influenced by a moving mass. One of the contributions of his paper was to investigate the separation of a moving load from the beam while it is traveling on the beam through controlling and computing the contact force between them. Once again the mass magnitude and velocity of movement of the load on the Timoshenko beam were found as two most important parameters determining the dynamic behavior of the beam [6]. Nikkhoo et al. [7] used the eigenfunction expansion method to analyze an Euler-Bernoulli beam when influenced by a moving mass. The method was employed to solve the governing differential equations. In that study a critical velocity was defined as the ratio of span's length and the first period of the structure. The results of that paper shows that for velocities beyond critical value the full acceleration terms must be considered for the dynamic equations. Similar papers were published after applying the abovementioned results [8, 9]. A simply supported beam acting upon a moving inertia load was investigated by Rao [10]. He applied the mode superposition and multiple scale methods to solve the problem and concluded that the inertia term has a considerable effect on the dynamic response of the system. In another study, Wu et al. [11] investigated the dynamic behavior of a multi-span non-uniform beam influenced by a series of moving loads in the same and opposing directions, while the speed of loads is varying. Lee [12] studied the dynamic response of a beam excited by a moving load where the beam has several middle point constraints generated by linear springs. The method utilized in the paper was assumed the mode method. With a more practical approach, Chatterjee et al. [13] modeled a multi-span continuous bridge traversed by a moving load while the interaction between the load and the bridge is considered. In their problem, the vehicle was modeled as sprung or un-sprung masses. Ichikawa et al. [14] in a similar fashion to reference [7], used the method of eigenfunction expansion but this time for the multi-span beams. Once again, they testified the effect of inertia terms in evaluating the dynamic behavior of beam shape structures, especially when the values of mass weight and speed are increased. The work on the dynamic analysis of multi-span beams under moving mass were pursued by Kiani et al. [15]. They established the formulation of Generalized Least Square Method (GLSM) to solve the problem in the space coordinates. An interesting result was acquired, showing the effect of span's number in the vibration response of a beam, influenced by moving mass with a higher magnitude of velocity.

Free vibration of plates has been vastly investigated by many researchers during the few past years. Recently, Civalek [16] studied the free vibration of composite annular plates and cylindrical plates by the method of discrete singular convolution. He investigated the non-linear response of laminated plates with the aforementioned method [17]. The problem of vibratory plates acted upon moving loads or masses has been scrutinized by several researchers. Using the Finite Element technique, a rectangular Kirchhoff plate was investigated under an orbiting moving load by Cifuentes et al. [18]. In their study, the dynamic behavior of a plate's central point was analyzed and the deflection of the plate was shown through time history. One can easily see the importance of the effect of inertia on the dynamic response of plates for orbiting trajectory from that paper. The dynamic behavior of rectangular thin plates plus Euler-Bernoulli and Rayleigh beams were considered while acting upon a moving load by Gbadyan et al. [19]. The modified generalized finite integral transforms and Struble were two methods applied in the paper to solve the governing differential equations. In that work, the path of moving load was assumed to be parallel with the edges of the plate and the results were presented within several time histories, computed at the plate's central point. The importance of inertia contribution in the dynamic response of the plate was emphasized again. In a dynamic analysis, Shadnam et al. [20] studied the behavior of a thin simply supported plate when it is forced to vibrate under a moving mass. The path of the load moving on the plate was assumed to be arbitrarily chosen. They used the

method of eigenfunction expansion to solve the equations of vibration. One of the most important results of their work is consideration of the effects of higher modes in the accuracy of computations and results. However, in a fashion similar to most previous studies they confined their formulation to apply the vertical component of acceleration.

Fryba [1] has presented the full term formulation of solids under moving loads and has discussed about the complexities of the problem when full term acceleration is considered. Nikkhoo et al. [21] analyzed the parametric study of a rectangular thin plate traversed by a moving mass. The mass traveled on an arbitrary path. They utilized the method of eigenfunction expansion to solve the plate's equation of motion. Within that article, having proceeded a parametric study, the effect of some parameters which could influence the dynamic behavior of the system were assessed. The essential conclusion that was pointed out from this paper was summarized in the necessity of inertia inclusion within the problem formulation. This was done to catch the accurate results, especially when the mass and velocity of the load movement is increased. Takabatake [22] investigated the vibration of a thin rectangular plate excited by a moving load through an analytical method. The plate has a variable thickness and the solution procedure uses the characteristic function. Huang et al. [23] developed a procedure for analyzing a plate resting on an elastic foundation traversed by a moving mass by using the finite strip method. In another study, Ghazvini et al. [24] presented a computational procedure and they assessed the dynamic behavior of a rectangular plate with variable thickness when it is acted upon by a moving mass using the eigenfunction expansion method. Nikkhoo et al. [25] investigated the dynamic behavior of rectangular plate excited by series of moving masses by using a semi-analytical method. They utilized the eigenfunction expansion method to solve the differential equation of motion. A Mindlin plate under distributed moving mass excitation was analyzed using finite difference procedure by Gbadyan et al. [26]. In another paper about the Mindlin plates, Amiri et al. [27] investigated the dynamic response of thick plates traversed by a moving mass based on first-order shear deformation theory using separation of variable as well as the eigenfunction expansion method, simultaneously. Eftekhari et al. [28] investigated the vibration of rectangular plates under accelerated moving loads. They employed several applications of Ritz, differential quadrature and integral quadrature methods. The Ritz method was used to separate the spatial partial derivatives while the differential quadrature method and integral quadrature method were applied to simulate the system's partial differential equations and finally the numerical method of Newmark was employed to solve the ordinary differential equations. Wu [29] studied a moving load traveling on a circular trajectory on the plate's surface causing vibratory behavior for the system. Moreover, Wu [30, 31] used the finite element method to analyze the dynamic response of an inclined plate traversed by a moving distributed load. The vibration analysis of a plate excited by a moving concentrated mass using an equivalent finite element procedure was performed by Esen [32].

Recently a comprehensive investigation on a thin plate vibrated by a moving load (force and mass) with arbitrary boundary conditions was performed by Song et al. [33]. In that study the governing differential equations were derived using the Lagrange equation and the updated Rayleigh-Ritz method associated with courant's penalty was employed in order to deal with the spatial partial derivatives. The admissible functions just satisfy a totally unconstrained condition. Then the differential quadrature method was used for discretization of the temporal derivatives.

Solution of multi-span plates involves complex differential equations of motion with partial derivatives with respect to two spatial components and another temporal variable. On the other hand, the existence of solution in free and forced vibration analysis of these plates greatly depends on boundary conditions. In the literatures, the analytical solution has often been presented for two opposite simply supported edges of plates in most complex conditions [34]. Because of these complexities in the problem formulation and solution, less attention has been paid to this important and practical problem thus far.

The free-edge boundary conditions are classified into natural types
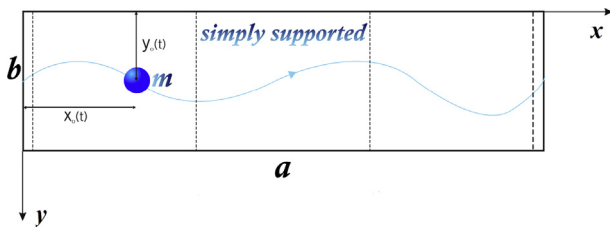
Fig. 1. Schematic of multi-span plate with simply supported constraints in width and free-edge in length direction acted upon a load traveling on an arbitrary trajectory.
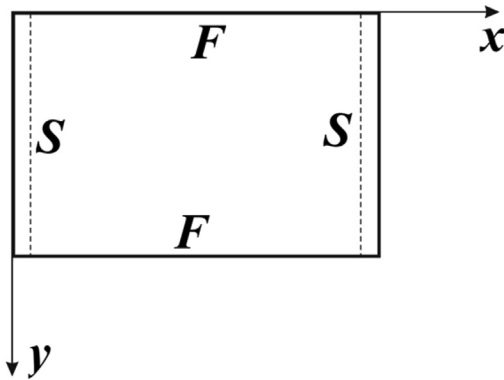
Fig. 2. A single-span plate with free-edge in longitudinal edges and simply supported along width, SFSF.

Fig. 3. Fundamental polynomials for 2D domains in triangle arrangement (Pascal's triangle).

(Newman) which result in more difficulties into the analytical procedures. Thus, numerical methods have been utilized in most studies to handle such plates in vibrating behavior.

Considering the aforementioned literature review, and with an attempt to compensate for the lack of sufficient analysis of continues plates, we investigate a thin multi-span plate under excitation of a concentrated moving load on an arbitrary trajectory which has not been assessed so far should.

The problem formulation is presented for moving inertia mass,

including the full terms of convectional acceleration components. The middle supports are proposed to satisfy simply supported conditions and the longitudinal edges will be free from constraints. The Hamilton's principle is utilized to derive the governing partial differential equations of motion, and then the Galerkin method is used to solve the problem in general form to separate the variables into spatial and temporal ones, within the proposed solution function. Mode shapes are generated by the Boundary Characteristic Orthogonal Polynomials (BCOP) method in a novel application of the method, through this article to create the vibrational mode shapes of multi-span plates for the first time (based on authors' literature review). A free vibration analysis is performed and the frequency as well as the fundamental period of structure would be derived, consequently. This is straightforwardly obtained by a standard eigenvalue. The results of free vibration analysis for two and three-span plates are reported in the tables which show a very good convergence for the frequency parameter, increasing the number of computational modes to 62. It could testify the accuracy of the procedure. The robust Matrix Exponential Method (MEM) is employed to derive the solution in the time domain such the complete solution is obtained.

A comprehensive parametric study is performed for investigation of the Dynamic Amplification Factor (**DAF**) at the point of first and second mid-span of single, two and three-span plates, when it is excited by a moving mass with constant velocity travelling on a path parallel to the longitudinal edges.
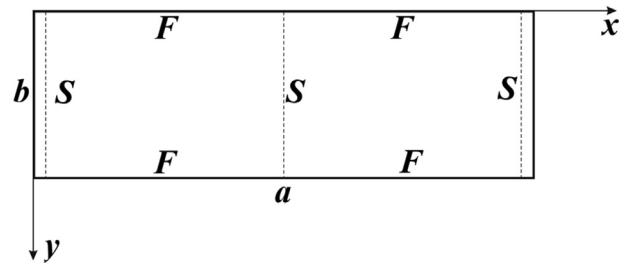
Fig. 4. Schematic for two-span plate with simply supported constraint at the middle of the length. Two longitudinal edges are free and the ends of the plate are simply supported, SFSF.
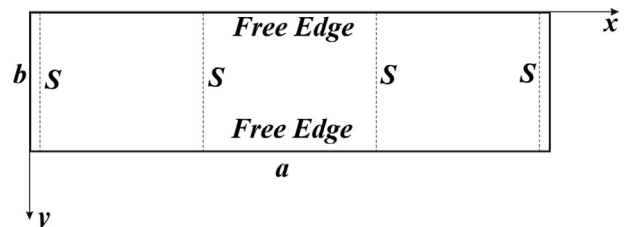
Fig. 5. Schematic of a three-span plate with middle simply supported constraints and equal length of spans. Two longitudinal edges are free and both ends are simply supported, SFSF.

Table 1
Convergence evaluation of the first-five frequency parameters and corresponding period of vibration derived from the BCOP method for two-span square plate, while the number of computational modes have increased.

Number of modes, N	20	25	35	40	50	62
λ_1 (rad/s)	38.9719	38.9699	38.9459	38.9459	38.9449	38.9449
T_1 (sec)	0.023840	0.023841	0.023856	0.0238564	0.023857	0.0238570
λ_2 (rad/s)	47.1331	46.7643	46.7484	46.7388	46.7388	46.7381
T_2 (sec)	0.019712	0.019867	0.019874	0.019878	0.019878	0.019879
λ_3 (rad/s)	62.3754	62.3754	61.7092	61.7092	61.4923	61.4913
T_3 (sec)	0.014895	0.014895	0.015056	0.015056	0.0151094	0.0151096
λ_4 (rad/s)	72.0533	68.9179	68.5770	67.8902	67.8351	67.5784
T_4 (sec)	0.012894	0.013481	0.013548	0.0136855	0.013696	0.01374
λ_5 (rad/s)	72.0533	71.9619	70.7810	70.7806	70.7406	70.7402
T_5 (sec)	0.012894	0.012911	0.013126	0.013126	0.013134	0.013134

Table 2

Convergence evaluation of the first-five frequency parameters and the corresponding period of vibration derived from BCOP method for three-span square plate, while the number of computational modes are increased.

Number of modes, N	20	25	35	40	50	62
λ_1 (rad/sec)	88.1918	88.1618	88.0101	88.0098	87.9881	87.9873
T_1 (sec)	0.010535	0.010538	0.010556	0.010556	0.010559	0.010559
λ_2 (rad/sec)	96.8765	96.2518	96.1118	96.0602	96.0601	96.0413
T_2 (sec)	0.0095906	0.009652	0.009666	0.009672	0.0096721	0.009674
λ_3 (rad/sec)	114.4536	114.4536	114.1902	114.1902	113.869	113.849
T_3 (sec)	0.008117	0.008117	0.0081365	0.0081365	0.008159	0.008160
λ_4 (rad/sec)	125.3994	121.9210	121.4019	121.3758	121.142	120.786
T_4 (sec)	0.007409	0.007620	0.007653	0.007654	0.007669	0.007692
λ_5 (rad/sec)	125.3994	124.4541	122.3336	122.3230	122.0552	122.043
T_5 (sec)	0.007409	0.007465	0.007594	0.007595	0.007612	0.007612
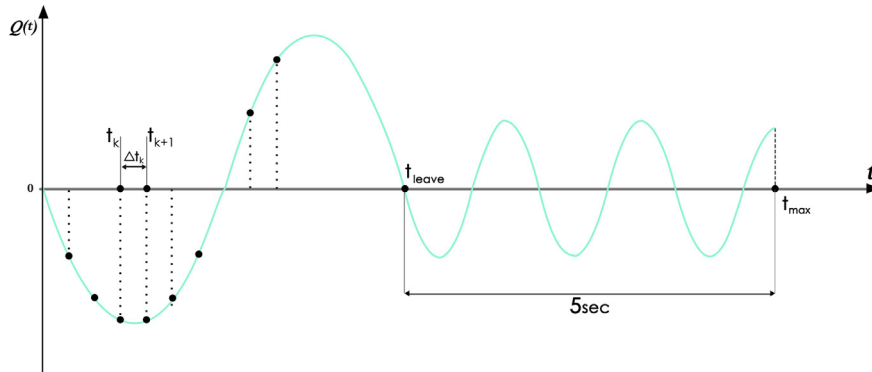
Fig. 6. Schematic for dynamic amplitude generation in time, for the plate under moving mass at mid-span.
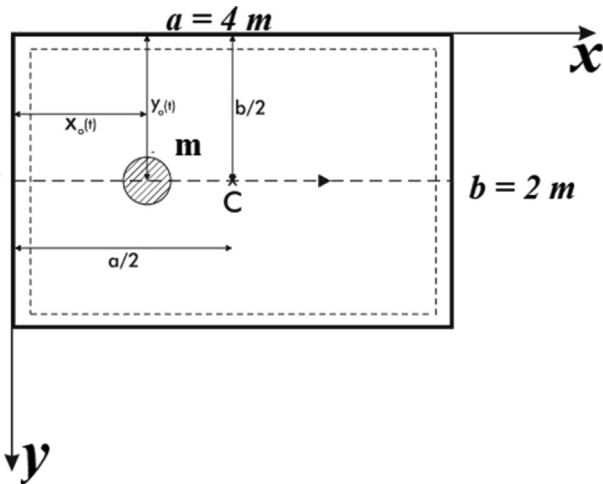
Fig. 7. Four edges simply supported single-span plate under moving mass with aspect ratio 2.

Finally, considering the fact that all computational results are performed for two cases with and without the effects of inertia within each numerical studies, a conversion factor, β, is introduced to show the difference between the responses for two abovementioned loading cases. It gives the possibility of solution for the problem in moving load conditions and finding the response of the plate under moving mass, subsequently.

2. Theory/calculation

2.1. Mathematical model

A thin rectangular multi-span plate is considered and the assumptions for Kirchhoff plates are established here. The mass per unit area, ρ, and $D = \frac{Eh^3}{12(1-\upsilon^2)}$ is its bending stiffness in which E, h, υ are the plate's modulus of elasticity, thickness of plate and Poisson's ratio respectively which assumed to be constant. This plate is excited by a moving inertia load rolling on the path which could be traced at each time by the variables x_0 (t) and y_0 (t), according to Fig. 1. Let $w(x,y,t)$ indicates the deflection of mid-plane points of plate with spatial coordinates x and y at any time of t. Also, initial conditions governing on the differential equations are represented by continues functions, $H_1(x,y)$ and $H_2(x,y)$, where $w(x,y,0) = H_1(x,y)$ and $\frac{\partial w(x,y,0)}{\partial t} = H_2(x,y)$. Considering the effects of inertia for moving load and keeping the small strain assumption, the equation of motion governing on the excited plate in the partial form using Hamilton's principle becomes:

$$D\nabla^4 w + \rho \frac{\partial^2 w(x,y,t)}{\partial t} = m\left(-g - \frac{d^2 w_0(t)}{dt^2}\right)\delta(x - x_0(t))\delta(y - y_0(t)) \quad (1)$$

Within Eq. (1), the parameters m, g, δ, and $w_0(t)$ are defined as the mass magnitude travelling on the plate, gravity acceleration, Dirac-delta

$$\frac{d^2 w_0(t)}{dt^2} = \left\{ \frac{\partial^2 w}{\partial t^2} + \frac{\partial^2 w}{\partial x^2}\left(\frac{dx}{dt}\right)^2 + \frac{\partial^2 w}{\partial y^2}\left(\frac{dy}{dt}\right)^2 + 2\frac{\partial^2 w}{\partial x \partial y}\left(\frac{dx}{dt}\right)\left(\frac{dy}{dt}\right) + 2\frac{\partial^2 w}{\partial x \partial t}\left(\frac{dx}{dt}\right) + 2\frac{\partial^2 w}{\partial y \partial t}\left(\frac{dy}{dt}\right) + \frac{\partial w}{\partial x}\left(\frac{d^2 x}{dt^2}\right) + \frac{\partial w}{\partial y}\left(\frac{d^2 y}{dt^2}\right) \right\}_{\substack{x = x_0(t) \\ y = y_0(t)}} \quad (2)$$
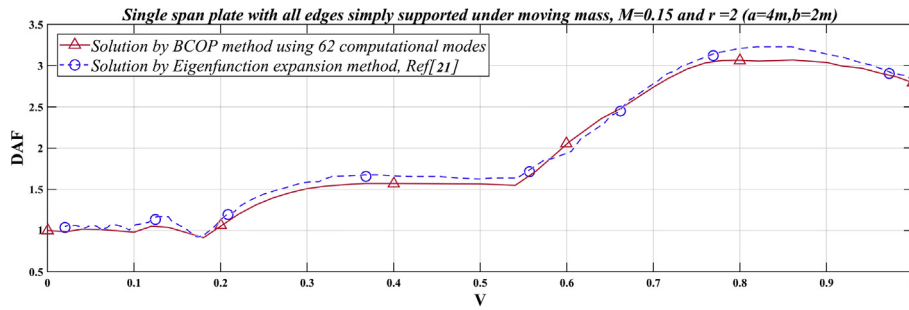
Fig. 8. A comparison between analytical and numerical methods of eigenfunction expansion and BCOP, respectively. The case study is a single-span simply supported plate, SSSS, under moving mass with mass ratio *0.15*, and aspect ratio *2(a=4m, b=2m)*.
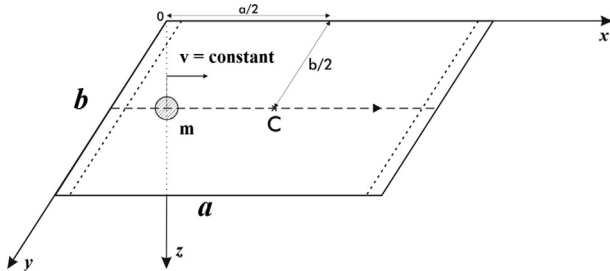
Fig. 9. 3D schematic for single-span plate with SFSF boundary conditions under moving load traveling on a rectilinear path with constant velocity. The dashed line shows simply supported and the other sides are free from constraint.

Table 3
Fundamental period of single-span plate with SFSF boundary condition for three values of aspect ratio *1, 2* and *3*.

Aspect ratio, r	1(a=2m,b=2m)	2(a=4m,b=2m)	3(a=6m,b=2m)
Fundamental period of plate, T_1	0.097	0.391	0.891

function and a variable which indicates the displacement of mass at any time of t in direction of *z-axis*, respectively.

In addition, to comply to the condition of pure rolling between the mass and the plate, assuming that they never loose contact, the following expression must be satisfied, $w_0(t) = w(x_0(t), y_0(t))$.

Expanding the time derivate of $w_0(t)$ yields to:

In the exact and complete formulation, all of the convective terms in Eq. (2) are considered. In order to solve Eq. (1), the Galerkin method in a general form is applied, to separate the spatial and temporal functions. So we can consider the following form of deflection function of the plate as below:

$$w(x, y, t) = \sum_{j=1}^{N} \varphi_j(x, y) Q_j(t) \tag{3}$$

In Eq. (3), the mode shape functions are indicated by $\varphi_j(x,y)$, which would be made by Boundary Characteristic Orthogonal Polynomials (BCOP) [33] that must satisfy the geometrical boundary conditions as well as comply with the orthogonality properties for all mode shapes. The mode shapes are created through the BCOP method by employing the Gram-Schmidt procedure to establish the orthogonality between terms. $Q_j(t)$ is the time dependent modal amplitude of the plate which would describe the time variation of any point of the plate located at the middle surface. Solution in the time domain would be derived aided by the state space formulation of the problem at first, and solving the temporal equations through the Matrix Exponential Method (MEM), consequently.

2.2. Gram-Schmidt orthogonalization procedure

Let a series of functions like $f_i(x)$ is given. By the well-known Gram-Schmidt orthogonalization procedure, one can generate a set of appropriate orthogonal functions following the steps below:

$$\begin{aligned}
\varphi_1 &= f_1 \\
\varphi_2 &= f_2 - \alpha_{21}\varphi_1 \\
\varphi_2 &= f_3 - \alpha_{31}\varphi_1 - \alpha_{32}\varphi_2
\end{aligned} \tag{4}$$

In which,

$$\alpha_{21} = \frac{<f_2, \varphi_1>}{<\varphi_1, \varphi_1>} , \ \alpha_{31} = \frac{<f_3, \varphi_1>}{<\varphi_1, \varphi_1>} , \ \alpha_{32} = \frac{<f_3, \varphi_2>}{<\varphi_2, \varphi_2>} , \dots \tag{5}$$

Briefly, one can use the summation representation as below:

$$\begin{aligned}
\varphi_1 &= f_1 \\
\varphi_i &= f_i - \sum_{j=1}^{N} \alpha_{ij}\varphi_j
\end{aligned} \tag{6}$$

where,

$$\alpha_{ij} = \frac{<f_i, \varphi_j>}{<\varphi_j, \varphi_j>} = \frac{\int_a^b w(x)f_i(x)\varphi_j(x)dx}{\int_a^b w(x)\varphi_j(x)\varphi_j(x)dx} \tag{7}$$

Through Eqs. (4), (5), (6), and (7), φ_j's, denote the proposed orthogonal functions generated by original set of f_i's. In addition $w(x)$ is the weight function in which the common shape of isotropic plates with constant thickness could be taken as unity. This procedure could be developed into *N*-dimensional spaces, where a plate could be categorized as a special case with two-dimensional variables.

2.3. Boundary Characteristic Orthogonal Polynomials (BCOP)

Although the Rayleigh-Ritz method is an efficient and applicable approach in dynamic analysis problems, there are some challenges in the use of mode shape functions in the method. Using the orthogonal functions specifically polynomials in the above mentioned method leads to considerable simplifications and yields a straightforward solution. The mode shapes are utilized in the Rayleigh-Ritz method as a linear combination of functions as mentioned before and must at least meet the geometrically boundary conditions at least. Considering this fact and surveying the literature, it could be pointed out that many various functions could be employed to reflect the vibrational modes of the system. Here, we are going to apply orthogonal polynomials in vibration analysis of multi-span plates under moving loads. These polynomial functions in a general form could be generated by Gram-Schmidt procedure, initiated by a linear independent series of substantial polynomials with single variable, such as 1, x, x^2, x^3, …. In addition, the procedure could be proceeded by well-known triangle 1, x, y, x^2, xy, y^2, for two-dimensional domains …. . Bhat (1978) utilized polynomials with two variables to analyze the dynamic behavior of plates through the Ritz

(a)

(b)

(c)
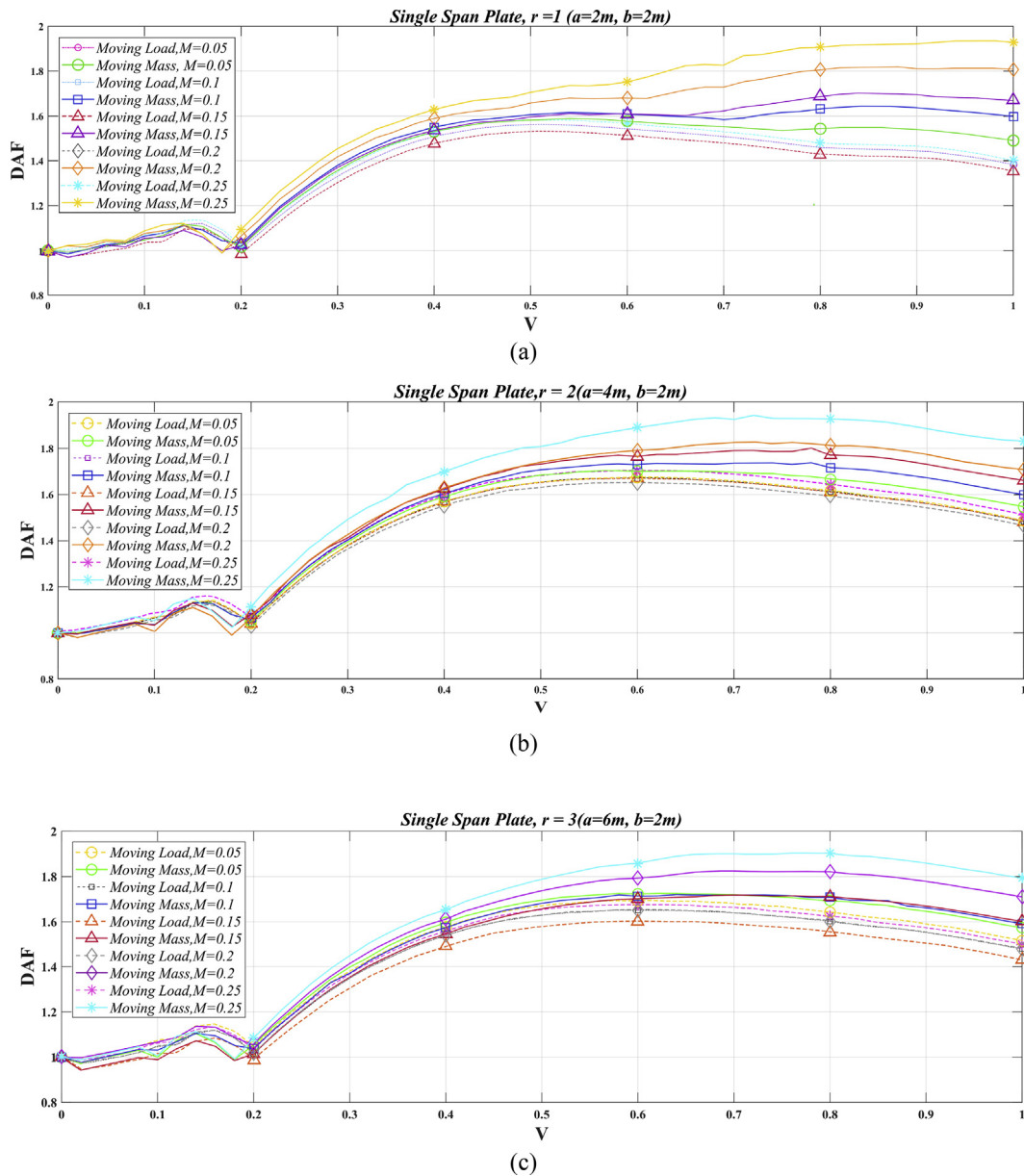
Fig. 10. Investigation of the mass ratio parameter, *M*, for single-span plate with SFSF boundary condition. Each graphs denotes the Dynamic Amplification Factor, **DAF**, versus non-dimensional velocity, **V**, calculated at middle of the plate's span. (a) *r = 1*, (b) *r = 2* and (c) *r = 3*.

method. However, in Bhat's procedure the boundary conditions were met just for the first mode and the method lacked sufficient accuracy in higher natural frequencies at higher computational. Chakraverty et al. [35] overcame this problem by applying a new approach for orthogonal polynomials such that the boundary conditions were satisfied over all mode shapes using a geometrical function pre-multiplied into the other. So because of the existence of this function, all terms of mode shapes satisfy the geometrical boundary conditions beyond having the orthogonality advantages.

2.3.1. BCOPs for single-span plates

A rectangular plate is a special case of parallelogram domains where the angle between each two sides are *90°*. Therefore, the below transformation could be applied in order to get the non-dimensional form of coordinates

$$x = a\xi + (b\cos\alpha)\eta$$
$$y = (b\sin\alpha)\eta$$
(8)

Eq. (8) includes terms which transform the original coordinates, *x-y*, into a unit square, $\xi - \eta$, domain. It has to be noted that by taking the inverse transform, one can easily generate the mode shapes in the original coordinates.

Based on the independent linear set of functions in $\xi - \eta$ coordinates, $f(\xi, \eta) = \{1, \xi, \eta, \xi^2, \xi\eta, \eta^2, \xi^3, \xi^2\eta, \eta^3, \dots \}$, we can start to generate the mode shapes over a unit square through the transformation $x = a\xi$, $y = b\eta$, where, *a* and *b* are the length and width of the plate, respectively. Finally, the mode shapes in original coordinates could be derived by the above transformation in the inverse form. So, we can write Eq. (9) for a plate as follows:

$$g(\xi, \eta)\{1, \xi, \eta, \xi^2, \xi\eta, \eta^2, \xi^3, \xi^2\eta, \eta^3, \dots \}$$
(9)

In above expression $g(\xi, \eta)$, is a function which satisfies the geometrical boundary conditions and is defined as:

$$g(\xi, \eta) = \xi^p(1 - \xi)^q\eta^r(1 - \eta)^s$$
(10)

By assigning the values *0* and *1* to ξ and η within Eq. (10), one can define the edges of the transformed plate. Moreover, by giving the values of *0, 1* and *2* to the *p, q, r* and *s* all types of boundary conditions could be defined.

Fig. 2 shows a schematic of single-span plate with SFSF boundary

$$\left.\begin{array}{l} \varphi_1 = F_1 \\ \varphi_i = F_i - \sum \alpha_{ij}\,\varphi_j \\ \alpha_{ij} = \dfrac{< F_i,\ \varphi_j >}{< \varphi_j,\ \varphi_j >},\ j = 1, 2, \ldots,\ (j-1) \end{array}\right\} i = 2, 3, 4, \ldots \qquad (12)$$

conditions, denoting the simply supported and free edges alternatively.

Using the Gram-Schmidth procedure the BCOPs could be generated as Eq. (11) up to Eq. (13):

$$g(\xi, \eta) = \xi(1 - \xi) \qquad (11)$$

in which,

$$F_i = g(\xi, \eta) f_i(\xi, \eta) \qquad (13)$$

Moreover, $f_i(\xi, \eta)$ is chosen from linear independent series of functions which could be displayed as triangle scheme of Fig. 3:

Utilizing these BCOPs in the Rayleigh-Ritz method one can easily derive the frequency parameter through a straight forward procedure, calculated from the standard form of characteristic equation.

$$w(x, y) = \sum_{j=1}^{N} Cj\,\varphi_j \qquad (14)$$

$$\omega^2 = \frac{\iint_R \left[(\nabla^2 w)^2 + 2(1 - \nu)\left\{ w_{xy}^2 - w_{xx}w_{yy} \right\} \right] dxdy}{\rho h \iint_R w^2 dxdy} \qquad (15)$$

Eq. (14) proposes the general form of the solution where C_j's, are unknown coefficients and φ_j's represent the mode shapes of the plate. By replacing the functions in $\xi - \eta$ within Eq. (15), a standard eigenvalue
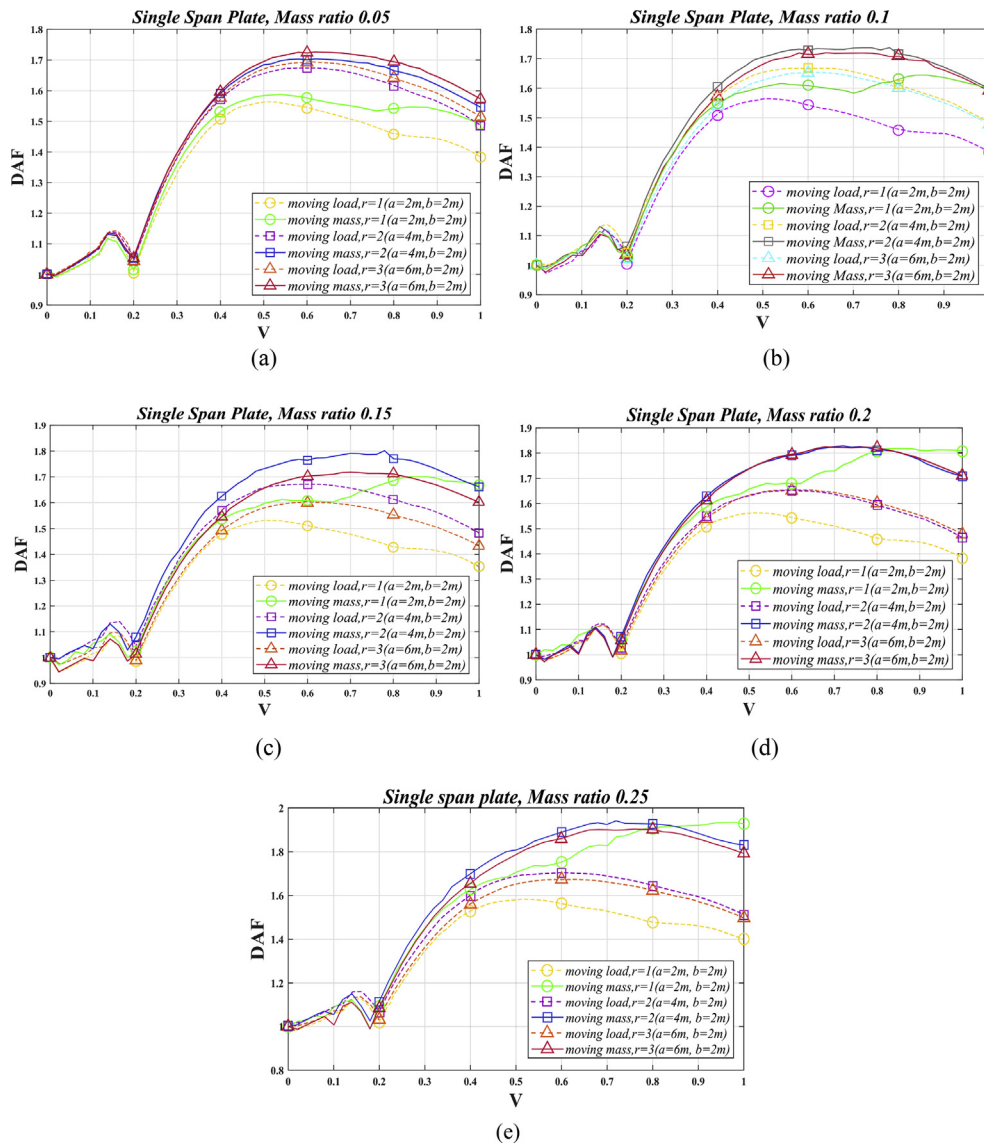
Fig. 11. Dynamic Amplification Factor, **DAF**, for single span SFSF plate calculated at mid-span, versus non-dimensional velocity, **V**, under moving load and mass when the aspect ratio changes within values *1, 2* and *3*. (a) *M = 0.05*, (b) *M = 0.1*, (c) *M = 0.15*, (d) *M = 0.2* and (e) *M = 0.25*.
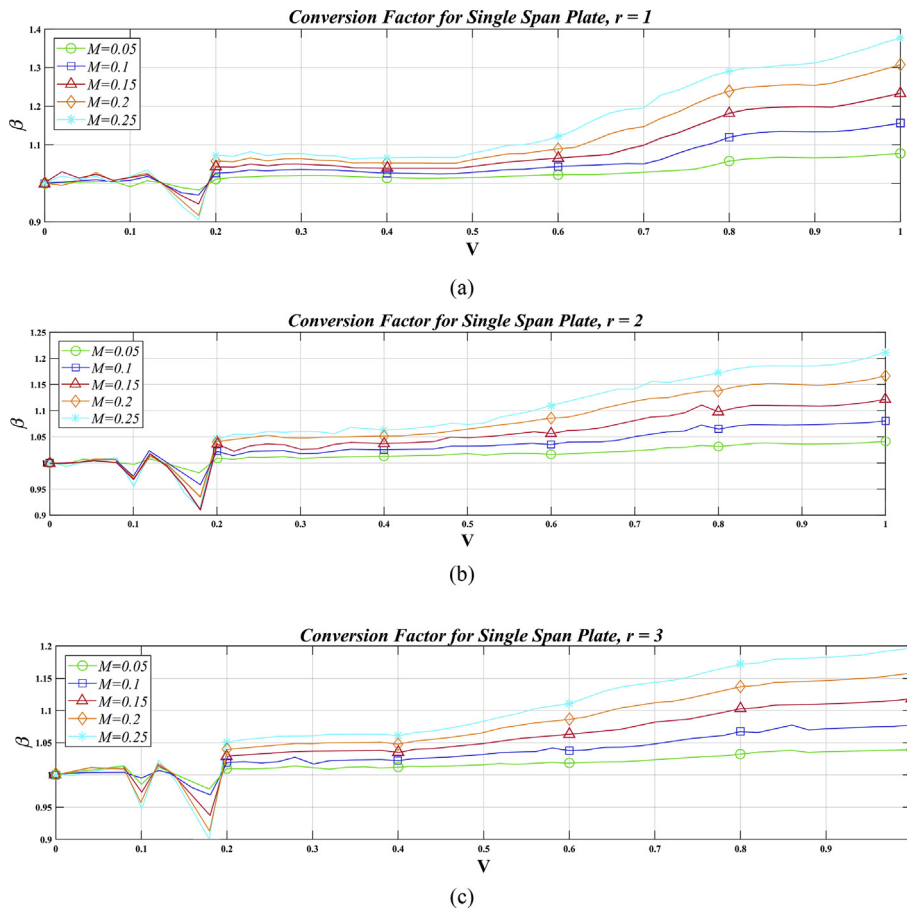
Fig. 12. The conversion factor, β, versus non-dimensional velocity, **V**, for single-span plate with SFSF boundary condition. The graphs are presented for constant aspect ratios *1*, *2* and *3*. (a) *r = 1*,(b) *r = 2* and (c) *r = 3*.
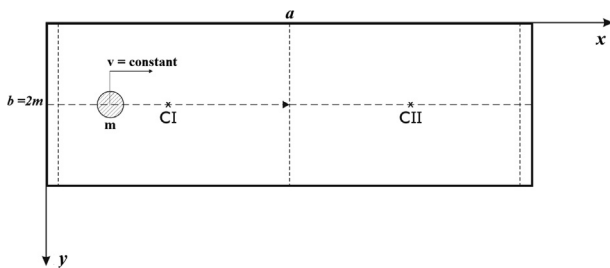
Fig. 13. Two-span plate under moving mass with constant velocity on the rectilinear path. The middle constraint is simply supported like two other supports on the ends of the plate and longitudinal edges of the plate are free from constraints.

Table 4
Fundamental period of two-span plate for three values of aspect ratios *1, 2* and *3*.

Aspect ratio, r	1(a=2m,b=2m)	2(a=4m,b=2m)	3(a=6m,b=2m)
Fundamental period of plate, T_1 (sec)	0.0239	0.097	0.22

equation could be derived as Eq. (16):

$$\sum_{j=1}^{N}\left(a_{ij} - \lambda^2 b_{ij}\right)Cj = 0 \qquad (16)$$

Where coefficients a_{ij} and b_{ij} are defined from Eq. (17) and Eq. (18):

$$a_{ij} = \iint_{R'}\left[\varphi_i^{\zeta\zeta}\varphi_j^{\zeta\zeta} + B_1\left(\varphi_i^{\zeta\eta}\varphi_j^{\zeta\zeta} + \varphi_i^{\zeta\zeta}\varphi_j^{\zeta\eta}\right) + B_2\left(\varphi_i^{\eta\eta}\varphi_j^{\zeta\zeta} + \varphi_i^{\zeta\zeta}\varphi_j^{\eta\eta}\right) + B_3\varphi_i^{\zeta\eta}\varphi_j^{\zeta\eta} \right.$$
$$\left. + B_4\left(\varphi_i^{\eta\eta}\varphi_j^{\zeta\eta} + \varphi_i^{\zeta\eta}\varphi_j^{\eta\eta}\right) + B_5\varphi_i^{\eta\eta}\varphi_j^{\eta\eta}\right]d\xi d\eta$$

$$(17)$$

$$b_{ij} = \iint_{R'}\varphi_i\varphi_j d\xi d\eta \qquad (18)$$

$$\lambda^2 = \frac{a^4\omega^2\rho h}{D} \qquad (19)$$

In Eq. (17), the superscripts indicate the derivatives with respect to the transformed variables ζ and η. In addition, Eq. (19) represents the square of the frequency parameter. The coefficients of $B_1,\ B_2,\ ...,\ B_5$ are defined within Eq. (20) up to Eq. (24) as below:

$$B_1 = -2r\,\mathrm{Cos}\,\alpha \qquad (20)$$

$$B_2 = r^2\left(\mathrm{Sin}^2\,\alpha + \mathrm{Cos}^2\,\alpha\right) \qquad (21)$$

$$B_3 = 2r^2\left(1 - v\,\mathrm{Sin}^2\,\alpha + \mathrm{Cos}^2\,\alpha\right) \qquad (22)$$

$$B_4 = -r^3\,\mathrm{Cos}\,\alpha \qquad (23)$$

$$B_5 = r^4 \qquad (24)$$

(a)

(b)

(c)
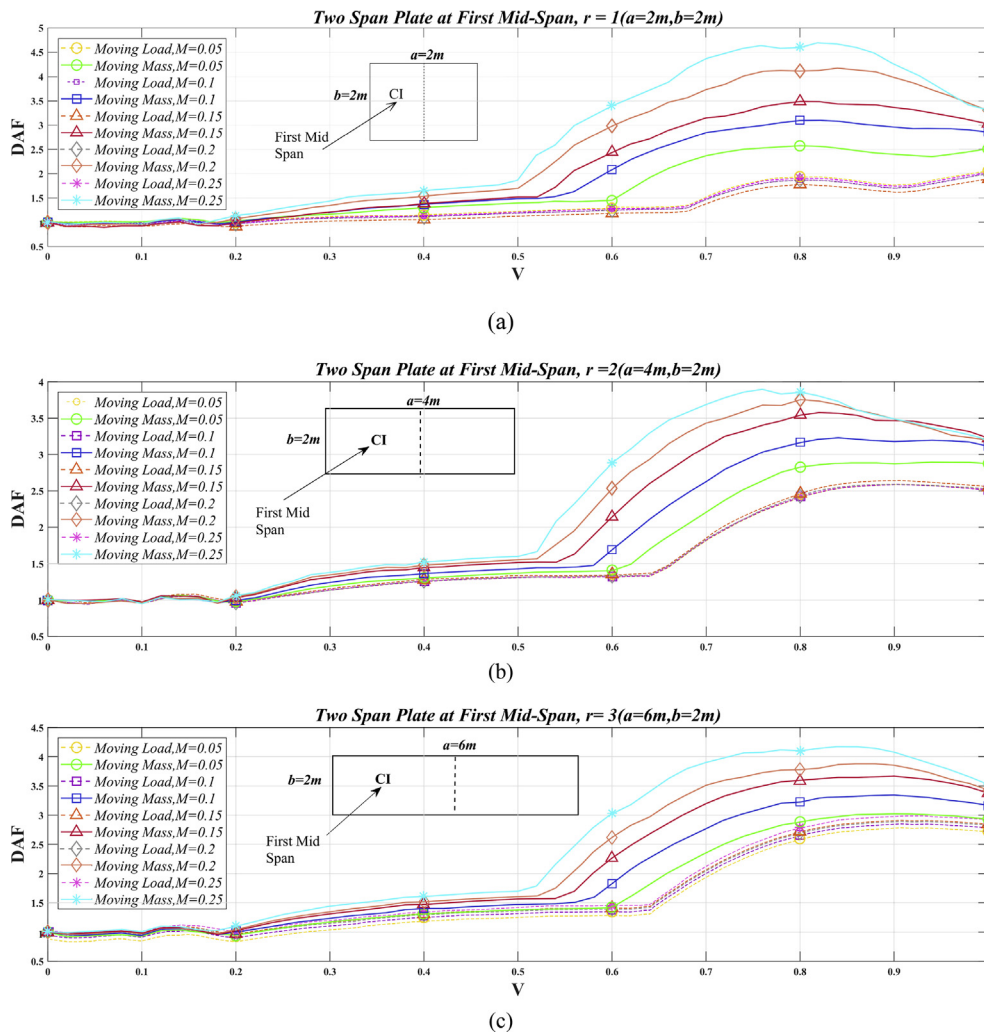
Fig. 14. The effect of moving mass velocity, **V**, on **DAF**, calculated at the first two-span plate's mid-span denoted by **CI**. Dashed lines are for moving load without inertia effect. (a) $r = 1$, (b) $r = 2$ and (c) $r = 3$.

$$r = \frac{a}{b} \tag{25}$$

Eq. (25) defines the aspect ratio parameter of the plate, r, and, α, denotes the angle between two edges of the plate where in the rectangular domains is $90°$. So, B_1 and B_4 would be omitted from the expressions.

2.3.2. Free vibration analysis of two-span plates by BCOP method

One of the most important features of the BCOP method in vibration analysis of plates is ease of use through the mode shape generation procedure, especially for multi-span plates. For the first time in this study, these polynomials are used for the dynamic analysis of two and three-span plates which undergo the moving inertia mass effects. Here, by defining the constraints in the middle of the plate and parallel to the width, one can easily create a two-span plate considering the fact that the BCOP method ensures satisfaction of the geometrical boundary conditions. A very good convergence for the frequency parameter is achieved as reported in Table 1 that indicates the accuracy of the method while the computational modes increase. Fig. 4 shows a schematic of a plate with two spans created by a simply supported constraint located at the middle of the length of the plate.

Similar to the previous section, after mapping the whole domain of plate into a unit square, we can define the middle support by taking the $g(\xi, \eta)$ function as Eq. (26):

$$g(\xi, \eta) = \xi(1 - \xi)\left(\frac{1}{2} - \xi\right) \tag{26}$$

which denotes a simply supported restraint on the line $\xi = \frac{1}{2}$. So, we can continue the procedure for 40 modes as shown in Eq. (27):

$$F_i(\xi, \eta) = g(\xi, \eta)\left\{1, \xi, \eta,\ \xi^2,\ \xi\eta, \ldots,\ \xi^5\eta^3\right\} \tag{27}$$

In a similar fashion the frequency parameter from Eq. (17) can be easily derived by using Eq. (10) and Eq. (12). The added constraint to the plate would cause to increase the stiffness of the system and it may substantially lead to the instability within the numerical computations. Thus, preserving the precision in the calculations has a very important role to boost the accuracy of the results and leads to prevention of numerical divergence. Considering this issue, we show the accuracy of the computations for a two-span plate in the free vibration analysis while the number of modes are increased to 62, according to Table 1. The results testify a very good convergence for the frequency parameter and period of vibration when the number of modes have increased, assuming the constant aspect ratio for plate, $r = 1$ ($a = 2m$, $b = 2m$), and Poisson ratio, $v = 0.3$.

2.3.3. Free vibration analysis of three-span plates by BCOP method

Fig. 5 depicts a typical three-span plate with two simply supported middle constraints located at equal distances from both ends of the plate.

In a similar manner by choosing an appropriate geometrical function, $g(\xi, \eta)$ as Eq. (28) one can conduct the procedure as follows:

$$g(\xi, \eta) = \xi(1 - \xi)\left(\frac{1}{3} - \xi\right)\left(\frac{2}{3} - \xi\right) \tag{28}$$

Again, after carrying out similar calculations for the frequency parameter derived from the standard eigenvalue problem, the first-five frequency parameters for a three-span plate with $r = 1(a = 2m, b = 2m)$ are listed in Table 2. There is a very important issue that could be considered as a strict evident on the precision of the procedure, which is a considerable trend of convergence as a result of calculations during the increment of modes contribution. Considering the fact that adding the constraints to each integrated structure such as plates leads to notable increased stiffness, having run the numerical computations for such stiffed structure, we expect to catch some numerical divergences specifically for higher computational modes. Nevertheless, not only was no divergence seen but also the convergence trend is interesting.

2.4. Matrix exponential method (MEM)

The solution in the time domain and deriving the function $\mathbf{Q}(t)$ is performed by a powerful iterative numerical method in the state space formulation called the Matrix Exponential Method (MEM) [34]. By substituting Eq. (3) into Eq. (1) and employing the orthogonality of modes one can rearrange the differential equation of motion for the plate in matrix form as follows:

$$\mathbf{M}(t)\ddot{\mathbf{Q}}(t) + \mathbf{C}(t)\dot{\mathbf{Q}}(t) + \mathbf{K}(t)\mathbf{Q}(t) = \mathbf{E}(t) \tag{29}$$

$$\mathbf{Q}(t_0) = \mathbf{Q}_0 \tag{30}$$

$$\dot{\mathbf{Q}}(t_0) = \dot{\mathbf{Q}}_0 \tag{31}$$

Eq. (29) up to Eq. (31) represent the matrix form of governing differential equations of motion where $\mathbf{Q}_0$ and $\dot{\mathbf{Q}}_0$ denote the initial conditions of the plate's vibration as the initial modal amplitude and initial modal velocity, respectively. All of the computations are performed for *40* computational modes. Thus, the mass, stiffness and damping matrices would be in the order of 40×40. The matrices could be calculated
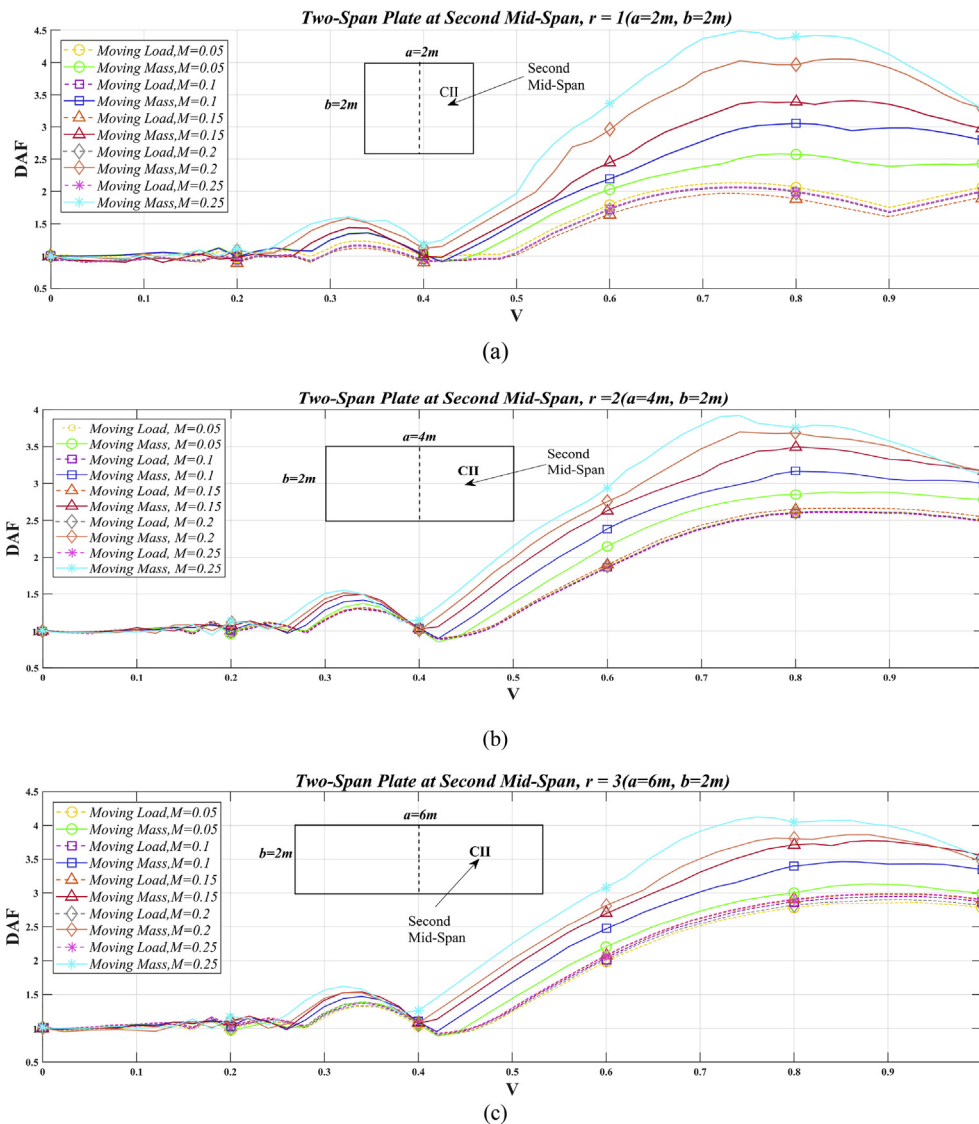
Fig. 15. The effect of moving mass velocity, **V**, on **DAF**, calculated at the second two-span plate's mid-span denoted by **CII**. Dashed lines are for moving load without inertia effect. (a) *r = 1*, (b) *r = 2* and (c) *r = 3*.

through the following expressions:

$$M_{ij} = m_{ij} + m\varphi_i(x_0(t), y_0(t))\left[\varphi_j(x_0(t), y_0(t)\right] \tag{32}$$

$$C_{ij} = 2m\varphi_i(x_0(t), y_0(t))\left[\dot{x}_0(t)\varphi_{j,x}(x_0(t), y_0(t)) + \dot{y}_0(t)\varphi_{j,y}(x_0(t), y_0(t))\right] \tag{33}$$

$$\begin{aligned} K_{ij} = k_{ij} &+ m\varphi_i(x_0(t), y_0(t))\left[\dot{x}_0^2(t)\varphi_{j,xx}(x_0(t), y_0(t)) + \dot{y}_0^2(t)\varphi_{j,yy}(x_0(t), y_0(t))\right. \\ &+ \ddot{x}_0(t)\varphi_{j,x}(x_0(t), y_0(t)) + \ddot{y}_0(t)\varphi_{j,y}(x_0(t), y_0(t)) \\ &\left. + 2\,\dot{x}_0(t)\dot{y}_0(t)\varphi_{j,xy}(x_0(t),\ y_0(t))\right] \end{aligned} \tag{34}$$

Where,

$$m_{ij} = \iint\limits_R \rho h\varphi_i(x,y)\varphi_j(x,y)dxdy \tag{35}$$

$$\begin{aligned} k_{ij} = \iint\limits_R &\left[D\,\frac{\partial^2 \varphi_i}{\partial x^2}\frac{\partial^2 \varphi_j}{\partial x^2} + \nu D\left(\frac{\partial^2 \varphi_i}{\partial x^2}\frac{\partial^2 \varphi_j}{\partial y^2} + \frac{\partial^2 \varphi_i}{\partial y^2}\frac{\partial^2 \varphi_i}{\partial x^2}\right) + D\frac{\partial^2 \varphi_i}{\partial y^2}\frac{\partial^2 \varphi_j}{\partial y^2}\right. \\ &\left. + 4\left(\frac{Gh^3}{12}\right)\left(\frac{\partial^2 \varphi_i}{\partial x\partial y}\frac{\partial^2 \varphi_j}{\partial x\partial y}\right)\right]dxdy \end{aligned} \tag{36}$$

$$D = \frac{Eh^3}{12(1 - \nu^2)} \tag{37}$$

$$E_j = -mg\varphi_j(x_0(t), y_0(t)) \tag{38}$$

Eqs. (32), (33), (34), (35), (36), (37), and (38) define components of mass, stiffness and damping matrices and the plate bending stiffness, D, is specifically presented by Eq. (37).

Having defined a state variable, $\mathbf{X}(t)$, according to Eq. (43), the state space representation of equation would be formulated as Eqs. (39), (40), (41), and (42).

$$\dot{\mathbf{X}}(t) = \mathbf{A}(t)\mathbf{X}(t) + \mathbf{F}(t) \tag{39}$$

$$\mathbf{A}(t) = \begin{bmatrix} 0 & \mathbf{I} \\ \mathbf{M}^{-1}\mathbf{K} & \mathbf{M}^{-1}\mathbf{C} \end{bmatrix}_{2N \times 2N} \tag{40}$$

$$\mathbf{F}(t) = \begin{bmatrix} 0 \\ -\mathbf{M}^{-1}E \end{bmatrix}_{2N \times 1} \tag{41}$$
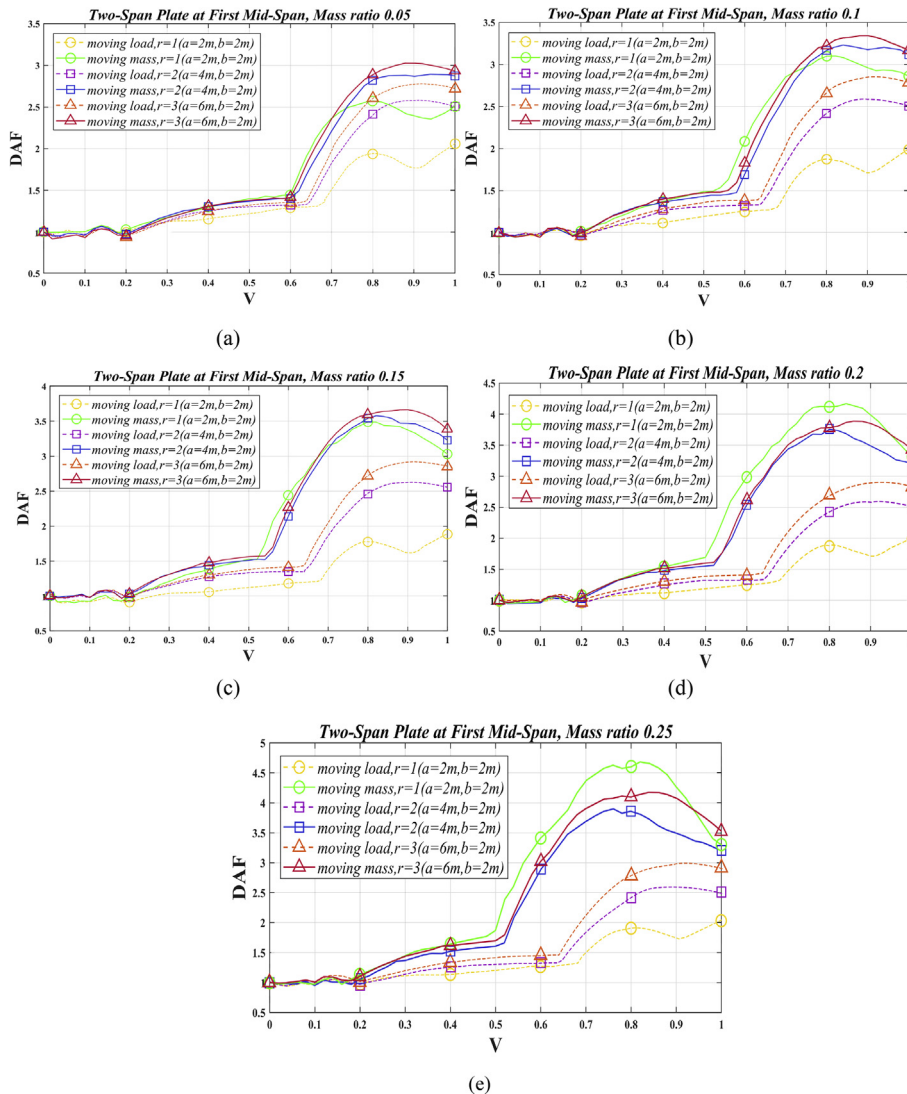
Fig. 16. Dynamic Amplification Factor, **DAF**, for two-span SFSF plate, calculated at the first mid-span, **CI**, versus non-dimensional velocity, **V**, under moving load and mass when the aspect ratio changes within values *1*, *2* and *3*. (a) *M = 0.05*, (b) *M = 0.1*, (c) *M = 0.15*, (d) *M = 0.2* and (e) *M = 0.25*.

$$\mathbf{Q}(t) = \begin{bmatrix} \mathbf{Q}_1(t) \\ . \\ . \\ . \\ \mathbf{Q}_N(t) \end{bmatrix}_{2N \times 1} \tag{42}$$

$$\mathbf{X}(t) = \begin{bmatrix} Q(t) \\ \dot{\mathbf{Q}}(t) \end{bmatrix}_{2N \times 1} \tag{43}$$

To implement the Matrix Exponential procedure [36], the following expression would be obtained assuming Eq. (44) as a solution matrix to Eq. (27), where $\mathbf{U}(t)$ is defined as a fundamental matrix:

$$\mathbf{X}(t) = \mathbf{U}(t)\mathbf{U}^{-1}(t_0)\mathbf{X}(t_0) + \int_{t_0}^{t} \left\{ \mathbf{U}(t)\mathbf{U}^{-1}(t)[\mathbf{F}(\tau)] \right\} d\tau \tag{44}$$

$$\dot{\mathbf{U}}(t) = \mathbf{A}(t)\mathbf{U}(t)\mathbf{X}(t_0), \ \mathbf{U}(t_0) = \mathbf{I} \tag{45}$$

$$\mathbf{X}(t) = \mathbf{U}(t)\mathbf{X}(t_0) \tag{46}$$

Eq. (45) and Eq. (46) denote the state space representation for $\mathbf{U}(t)$. Moreover, the transfer matrix is utilized to obtain $\mathbf{U}(t)$, such as Eq. (47) and Eq. (48):

$$\phi(t, \tau) \cong \mathbf{U}(t)\mathbf{U}^{-1}(\tau) \tag{47}$$

$$\mathbf{X}(t) = \phi(t, \tau)\mathbf{X}(\tau) \tag{48}$$

An approximate solution can be used to obtain $\mathbf{\Phi}$, where, $\phi(t_{k+1}, t_k) = e^{\mathbf{A}(t_k)\Delta t_k}$, in which $\Delta t_k = t_{k+1} - t_k$, that is a specific time interval. Assuming the existence of $\mathbf{A}^{-1}(t_k)$, Eq. (39) would be easily solved to yields. Eqs. (49), (50), (51):

$$\mathbf{X}(t_{k+1}) = \mathbf{A}_1(t_k)\mathbf{X}(t_k) + \mathbf{F}_1(t_k) \tag{49}$$

$$\mathbf{A}_1(t_k) \cong e^{\mathbf{A}(t_k)\Delta t_k} \tag{50}$$

$$\mathbf{F}_1(t_k) \cong [\mathbf{A}_1(t_k) - \mathbf{I}]\mathbf{A}_1^{-1}(t_k)\mathbf{F}(t_k) \tag{51}$$

By following the abovementioned steps, the partial differential equation is easily converted to an ordinary one in the time domain. Fig. 6 shows a diagram of dynamic amplitude in time. This Figure is actually a time history of the dynamic response of the plate which has been depicted for a specified point. The time interval in the numerical analysis is selected for values less than 0.002 sec. It has to be mentioned that the smoothness of the response curve and the precision of the result depends on the assigned Δt value, accordingly. Fig. 6 clarifies the numerical procedure which yields $Q(t)$, by substituting it into Eq. (3), the complete dynamic deflection would be obtained.

In Fig. 6, t_{leave} indicates the time that the mass has left the plate. Moreover, t_{max} denotes the time for the total numerical procedure. The free vibration phase starts just when the mass has left the plate at t_{leave},
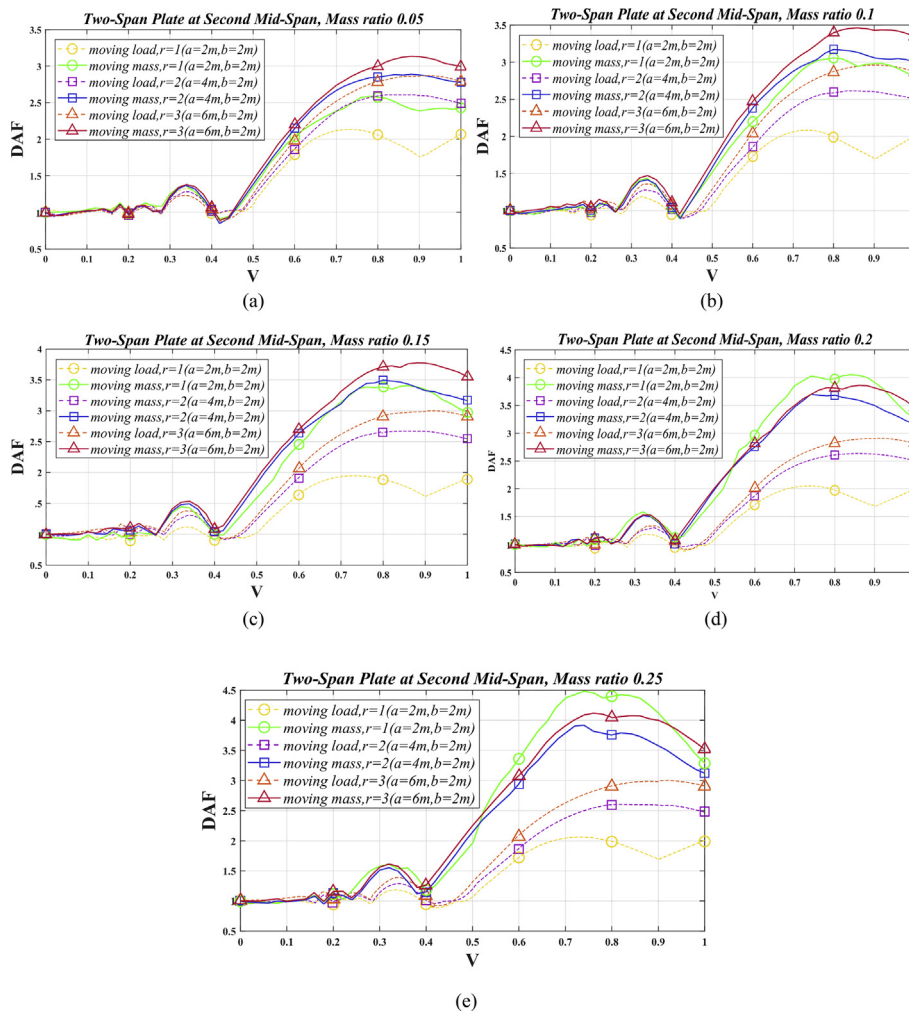
Fig. 17. Dynamic Amplification Factor, **DAF**, for two-span SFSF plate, calculated at the second mid-span, **CII**, versus non-dimensional velocity, **V**, under moving load and mass when the aspect ratio changes within values *1, 2* and *3*. (a) *M = 0.05*, (b) *M = 0.1*, (c) *M = 0.15*, (d) *M = 0.2* and (e) *M = 0.25*.

and it is proposed to take 5 sec in the numerical procedure.

The peaks of the parameter $Q(t)$, could depend on the velocity of mass which is traveling on the plate. We prolonged the computations into free vibrations for 5 sec, because in some cases the maximum of $Q(t)$ may occur in the free vibration phase. Multiplying this parameter by the mode functions derived from the BCOP method would yield a complete solution of partial differential equations.

The results within the next sections are presented in the non-dimensional form. This matter provides the possibility of extending the work to real-scale structures.
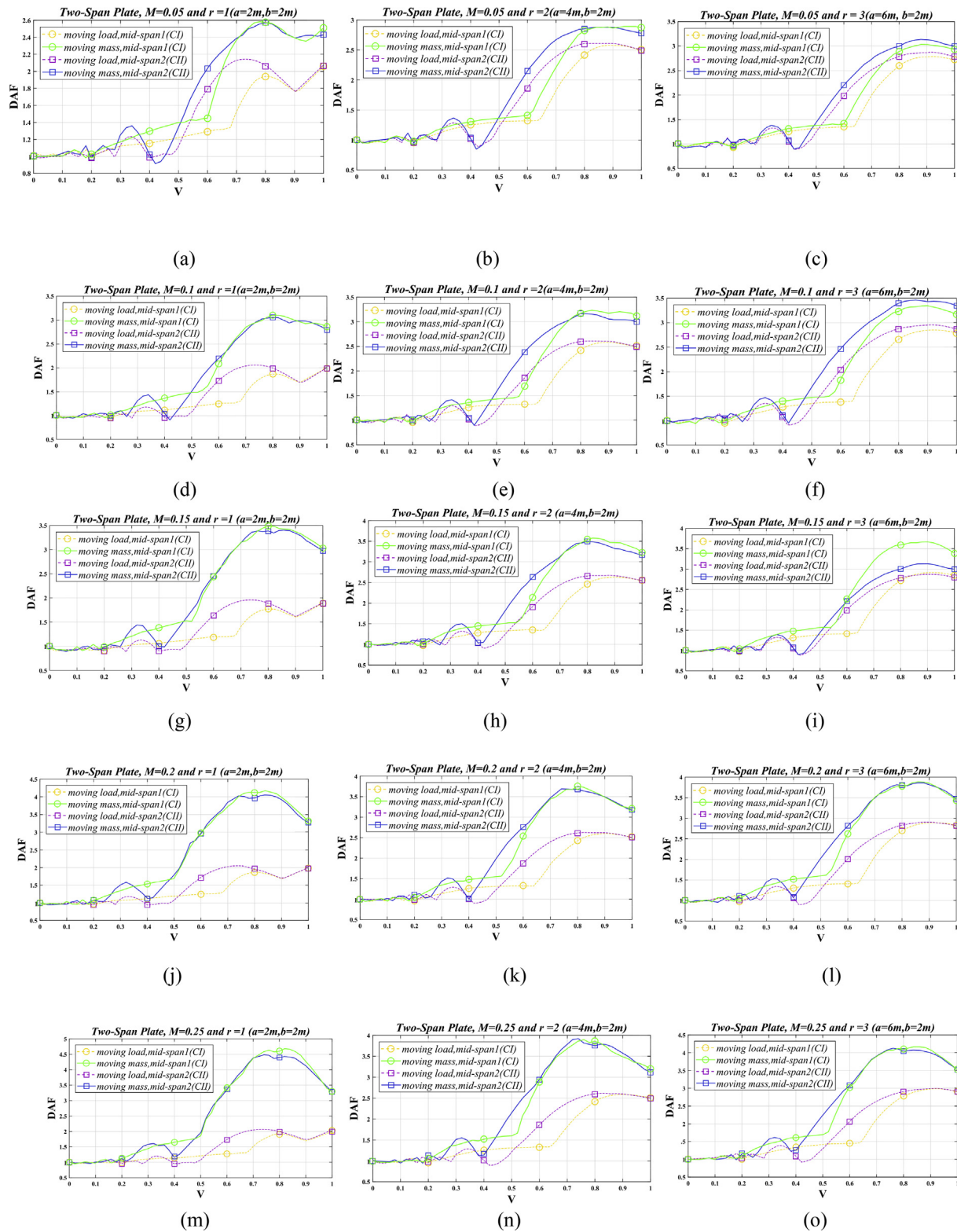
Fig. 18. The study on *reference point* (*CI* and *CII*) for two-span plate. Each Figure depicts **DAF** versus non-dimensional velocity, **V**, for constant mass and aspect ratio parameter. (a) *M = 0.05 & r = 1*, (b) *M = 0.05 & r = 2*, (c) *M = 0.05 & r = 3*, (d) *M = 0.1 & r = 1*, (e) *M = 0.1 & r = 2*, (f) *M = 0.1 & r = 3*, (g) *M = 0.15 & r = 1*, (h) *M = 0.15 & r = 2*, (i) *M = 0.15 & r = 3*, (j) *M = 0.2 & r = 1* (k) *M = 0.2 & r = 2*, (l) *M = 0.2 & r = 3*, (m) *M = 0.25 & r = 1*, (n) *M = 0.25 & r = 2*, (o) *M = 0.25 & r = 3*.

3. Results & discussion

This section is dedicated to analysis of three case studies including single-span plate, two-span and three-span plates are influenced by a moving inertia load. An Aluminum multi-span plate in a general form with material properties is considered as follows: modulus of elasticity $E=73.1$ GPa, mass density $\rho = 2700 \ kgm^{-3}$ and Poisson's ratio $v = 0.33$. The length of plate a, is varied so that several aspect ratios defined as $r = a/b$. It could be generated to use in parametric studies and would get values within *1, 2* and *3*. The width of the plate is assumed to be a constant, *2m*. The mass is traveling on the rectilinear path with constant velocity. It is also assumed that the plate is originally at rest and the pure rolling and full contact condition between the traveling mass and plate is met. Natural frequencies and mode shapes are derived by the aforementioned method in the previous sections. The magnitude of the mass weight is introduced by non-dimensional parameter as a ratio of the moving mass divided by total plate's mass, within *0.05, 0.1, 0.15, 0.2* and *0.25,* denoted by *M*. For instance, a mass ratio *0.2,* would be interpreted as *20* percent of the plate's mass which are travelling on the plate and determined as $M = m/\rho hab$, where h is the plate's thickness and has a constant value of 17 mm. The mass travels on the rectilinear path parallel to the length of the plate with constant velocity. The magnitude of the load's speed is presented by the non-dimensional parameter of speed and could be defined as $\mathbf{V} = v/v'$. v, is defined by $v' = 2a/T$, a parameter with dimension similar to velocity. We called it *reference velocity*. v', throughout this study, actually reflect the fundamental properties of

structures, including the length and the period of the plate. Because of this matter, v' could be appropriated to make a non-dimensional velocity, $\mathbf{V}$, varying between *0* to *1* [21]. The investigation on the dynamic response of the plate's central point is carried out by Dynamic Amplification Factor, **DAF**, defined as $DAF = \left|\dfrac{W_{max, \ dynamic}}{W_{static}}\right|$ in which $W_{max, \ dynamic}$ is the maximum dynamic deflection at the central point of the plate due to the dynamic effects of moving mass excitation, derived from a dynamic analysis. Moreover, W_{static}, is the deflection of the plate's central point has acted upon a static concentrated load at the same point. In the multi-span plates the *reference point* would be located at the middle span. Through a comprehensive parametric sensitivity study the effects of several non-dimensional parameters such as mass ratio, aspect ratio and the location of *reference point* would be investigated in the next sections. The results are presented in several graphs which could provide the readers with a complete behavior analysis of multi-span plates, denoting the spectra of **DAF** versus **V** for numerous case studies.

In every cases the problem is solved for both models of loading, when the inertia effects are included or ignored. This provides a comparison of the possibility for both loading conditions. It would be very useful especially for higher magnitude of velocities. In the two- and three-span plates, the **DAF**s of middle-span point are presented at the same graph to investigate the role and importance of the *reference point* in dynamic behavior of plate, once the moving load reaches it. In this paper, for two-span plates and three-span ones, **CI** and **CII** are the symbols to indicate the *reference point* locations for the first mid-span and the second mid-

(a)

(b)

(c)
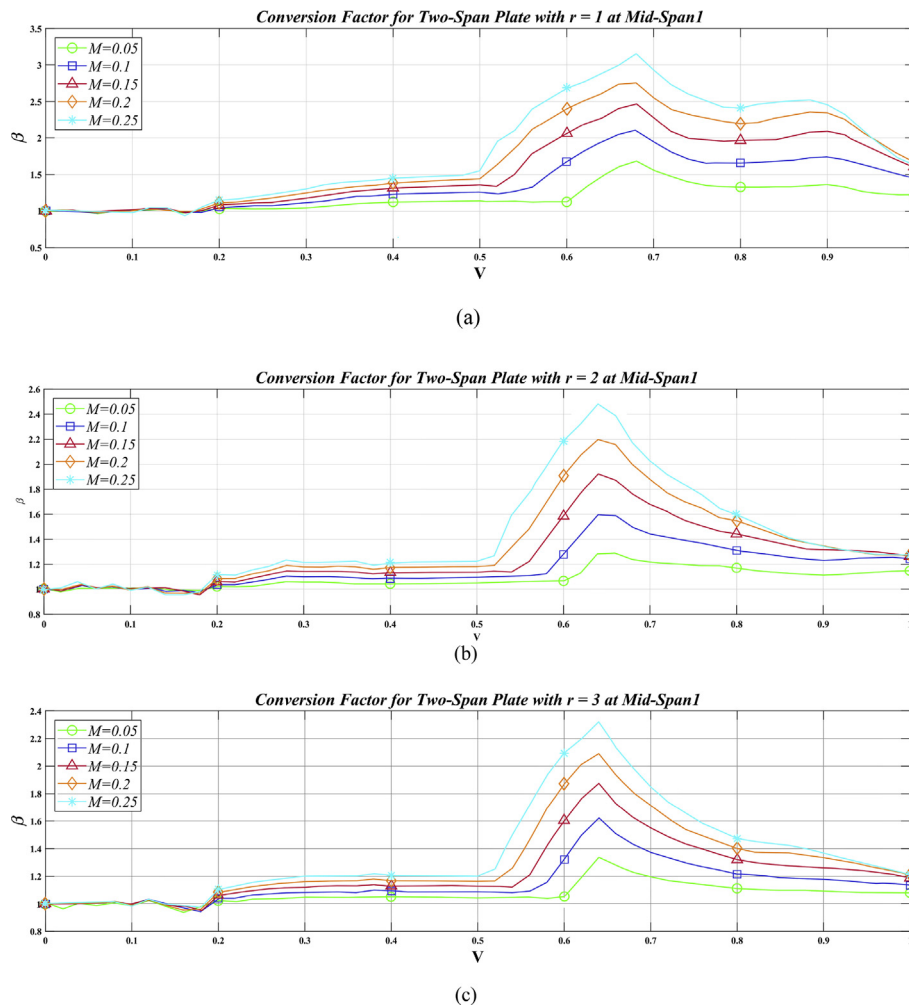
Fig. 19. Conversion factor for two-span plates with SFSF boundary condition versus non-dimensional velocity calculated at the first mid-span, **CI**, with specified mass and aspect ratios. (a) *r = 1*, (b) *r = 2* and (c) *r = 3*.

(a)

(b)

(c)
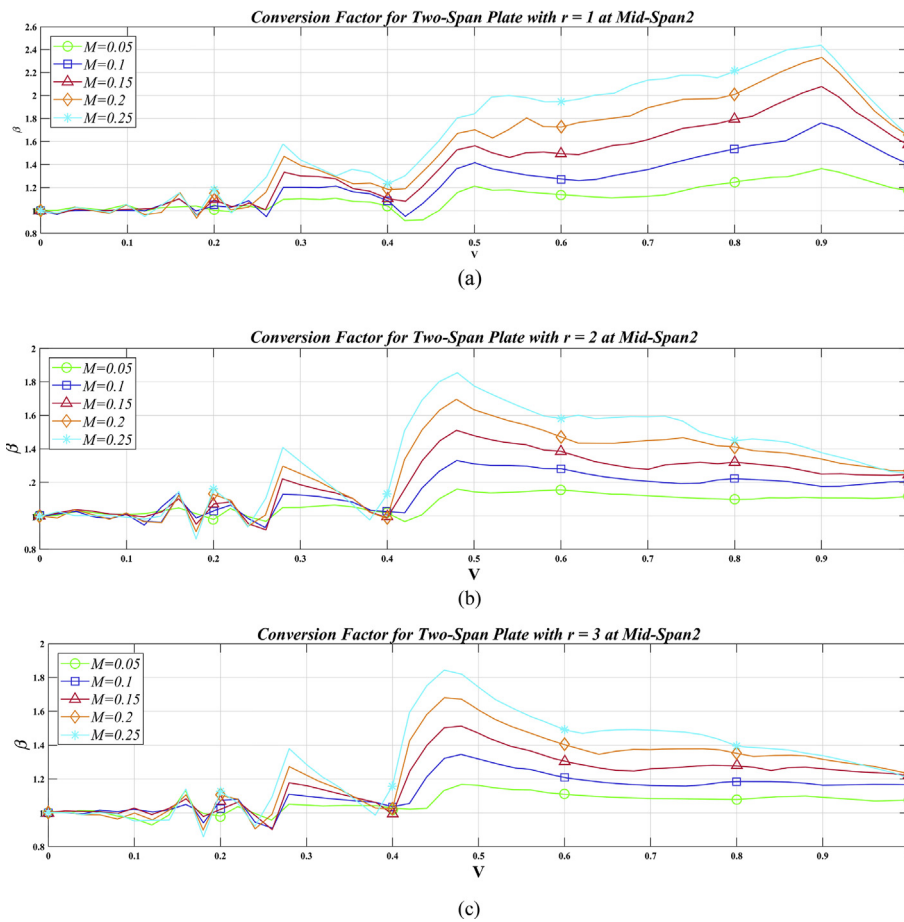
Fig. 20. Conversion factor for two-span plates with SFSF boundary condition versus non-dimensional velocity calculated at the second mid-span **CII** with specified mass and aspect ratio. (a) *r = 1*, (b) *r = 2* and (c) *r = 3*.

span, respectively. The plate before arrival of the moving load is assumed to be at rest, so the initial conditions is considered to be zero, $Q_0 = \dot{Q}_0 = 0$.

3.1. Verification

Dynamic analysis of a single-span simply supported plate under moving mass traveling on a rectilinear path was performed by Nikkhoo-Rofooei et al [21]. Several results were presented there using the eigenfunction expansion method in which the Dynamic Amplification Factor, **DAF**, was investigated for mass ratios versus the speed parameter, **V**. To perform a verification study a special case is selected here and solved by BCOP method to testify the accuracy of the procedure. The considered problem is a single-span plate with simply supported conditions over all the edges with aspect ratio *2 (a=4m, b=2m),* and the mass ratio *0.15*, the velocity of moving load is assumed to be constant when it is traveling on a rectilinear path. According to the aforementioned sections, the importance of analysis of plates under moving inertia mass would emerge more and more when the velocity of moving load is increased because the accuracy of numerical procedure would play an important role to capture the precise results in this situation. Based on these comments a very good and interesting result has been achieved that shows a satisfactory adaptation between the two methods of eigenfunction and BCOP, specifically at high speeds of moving load according to Fig. 7.

Fig. 8 shows a good agreement between the results derived from the methods of eigenfunction expansion and BCOP, specifically in the velocity parameters within *0.5* to *1*. The results strictly testify the numerical procedure's precision when the inertia effects of loading are involved and the full terms of acceleration considered into the formulation. Therefore, based on the acceptable verification presented, a comprehensive parametric study for single-span up to three-span plates can be established in subsequent sections, where for each one of the cases sensitivity analysis is carried out and the results are presented through corresponding graphs.
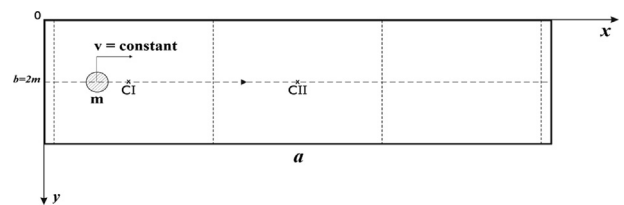
Fig. 21. A three-span plate under moving mass with constant velocity on the rectilinear path. The spans are generated by two middle simply supported constraints.

One can deduce useful information about every parameter which is

Table 5
Fundamental period of three-span plate for three values of aspect ratios *1, 2* and *3*.

Aspect ratio, r	1(a=2m,b=2m)	2(a=4m,b=2m)	3(a=6m,b=2m)
Fundamental period of plate, T_1	0.0106	0.0428	0.097

scrutinized within next sections through Tables and Figures. The boundary conditions assumed in the paper is simply supported, (**S**), to generate the spans, and free from constraint, (**F**), on the longitudinal sides.

3.2. Single-span plates

A thin rectangular single-span plate with the above mentioned conditions is considered. The moving load travels on the plate with constant velocity on a straight line parallel to the length of the plate according to Fig. 9. In addition, we can see the changes of the fundamental period of single-span plate derived from a free vibration analysis depending on aspect ratio value in Table 3.

3.2.1. The study on mass ratio parameter

The magnitude of mass ratio is investigated in this section for three values of aspect ratio. The presented graphs reflect the effect of mass magnitude on the Dynamic Amplification Factor of the plate's central point. For each constant aspect and mass ratio, it is seen that by increasing the speed of moving load the difference between load and mass plate's response would be increased. On the other hand, by increasing the mass weight in the constant aspect and speed ratio both the parameter **DAF** and difference between moving load and mass is increased. It is pointed out that the inertia effect must be considered in the analysis while the velocity is increased. Each one of the graphs of Fig. 9 consist of the curves of **DAF** versus non-dimensional velocity, **V**, for five mass ratios from *0.05* up to *0.25*, assuming the aspect ratio to be constant. On the other hand, the solution of the problem ignoring the

inertia effect for the aforementioned mass ratios are depicted in the graphs at the same time. This provides the other assessment of the results for the case of moving load. The dashed line through these graphs denotes the response of the plate acting upon a moving load, which means that the inertia effect has not been considered in the problem.

As it is shown in Fig. 10, the moving load condition can be used to predict the dynamic response of the system for moving mass velocities below $\approx 0.2\ v'$ and there is no need to consider the moving mass with the complexities that arise from the inertia terms. On the other hand, in velocities above $\approx 0.2\ v'$ the difference between the plate's response under moving load and mass has emerged. Then, the mass inertia effect must be considered. Moreover, studying mass ratio for the plate with a specific aspect ratio, it could be seen that the difference between the moving load and mass response of the system is increased at any velocity above $\approx 0.2\ v'$. Increasing the magnitude of mass weight traveling on the plate leads to the fact that inertia terms should be considered in the problem. Finally, upon evaluating the effect of aspect ratio we can deduce the difference between the response of the system under moving load and mass is decreased while the aspect ratio is increased. Therefore, the inertia effect of mass would be considered to be of less degree than the case with lower aspect ratio, specifically in the velocities near to $\approx 0.2\ v'$.

3.2.2. The study on aspect ratio parameter

Here, the effect of variation of aspect ratio parameter on the plate's response is investigated. So, the Figures show the **DAF** of plate's *reference point* versus non-dimensional velocity, **V**, including two cases of loading with and without the inertia effects of traveling mass at specific mass
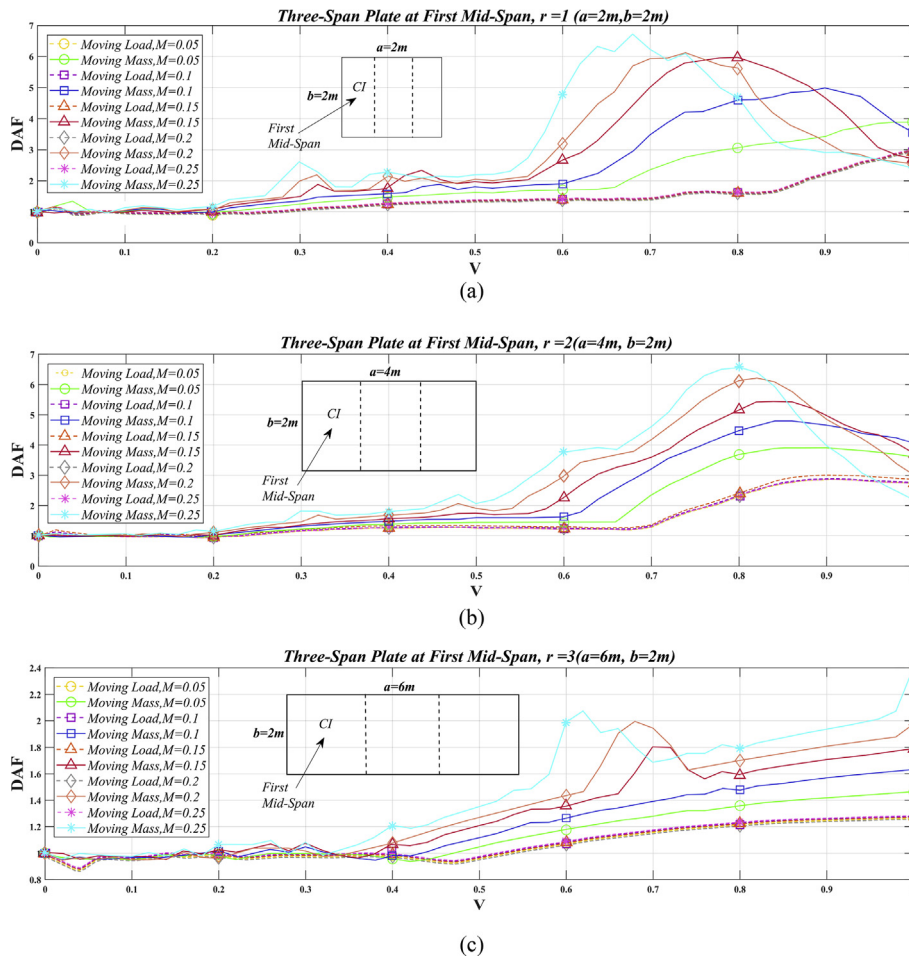
Fig. 22. The effect of moving mass velocity, **V**, on **DAF**, calculated at the first three-span plate's mid-span denoted by **CI**. Dashed lines are for moving load without inertia effect. (a) *r = 1*, (b) *r = 2* and (c) *r = 3*.

ratio.

It is pointed out that for each specified mass ratio, specifically at velocities above $\approx 0.2\ v'$and lower magnitude of mass weights, the difference between the response of the plate in load and mass moving on the plate shows a decreasing trend while the aspect ratio is increased. In other words, if one scrutinizes each Figure could easily find out that the most difference between the two cases of loading happens for square plates (*r =1*), by increasing the aspect ratio by *2* and *3,* this difference would be mitigated consequently. As an example, if we trace the behavior of **DAF** for a square plate with mass ratio *0.05,* an interesting trend is seen. Such that, at this specified mass ratio the trend of curve is increasing when the velocity parameter comes to$\approx 0.5\ v'$ at first, and starts to decrease by approaching$\approx 0.78\ v'$. Then the trend of the function suddenly changes to an increasing one from this velocity on. Thus, it could be seen that the highest effect of inertia occurs within the interval of$\approx 0.78\ v'$ up to the end. Following this manner, for square plates pertaining to the other mass ratios, it could be seen that while the mass ratio increases the velocity corresponding to the **DAF**'s peak $\approx 0.6\ v'$increased to $\approx 0.68\ v'$, keeping the aspect ratio *3*. As shown above, the gibes on the curves would happen in the lower speeds when the mass weight has increased. It means that the difference between the two curves starts to rise from the lower speed which emphasizes again on the importance of inertia effects for lager mass magnitude. Therefore, the interval of difference between the plate's response for the loading with and without inertia effects have remarkably increased. Therefore, in square plates one can conclude that the analysis of dynamic response must carry out considering the inertia mass, specifically for higher mass weights and

velocities (see. Fig. 11).

3.2.3. Conversion factor

One of the other investigations which has been carried out in this paper is dedicated to deriving and proposing a coefficient that assesses the trend of differences between both cases of loading, with and without the inertia effect of moving mass. Paying enough attention to this factor, one can easily find out that the problem must be solved for the inertia loading condition or not. For the simple cases in which the conversion factors, β is near to *1*, the problem could be solved without the inertia mass with a good accuracy. Thus, engineers have no need for enduring the complexities of mass inertia contribution to the differential equations. Moreover, in the cases that the coefficient goes far away from unity, it is possible to solve the problem in simple moving loads without considering the inertia effect. By multiplying the appropriate conversion factor into the response, the solution of moving mass is easily obtained.

Fig. 12 shows this factor for single-span plate versus non-dimensional velocity where a good and predictable trend is seen. Thus, one can apply a simple interpolation to derive a corresponding factor pertaining to the mass ratios which have values between the proposed quantities in the graphs.

The factor, β, is defined as $= \frac{DAF_{inertia\ mass}}{DAF_{load}}$. Fig. 12 contains three graphs, in which each one is presented for a specified aspect ratio.

Having acquired accurate results for single-span plates, we consider two and three-span plates and present the above mentioned studies with the same assumptions for material properties and boundary conditions in the following sections of the paper. All of the calculations are carried out

(a)

(b)

(c)
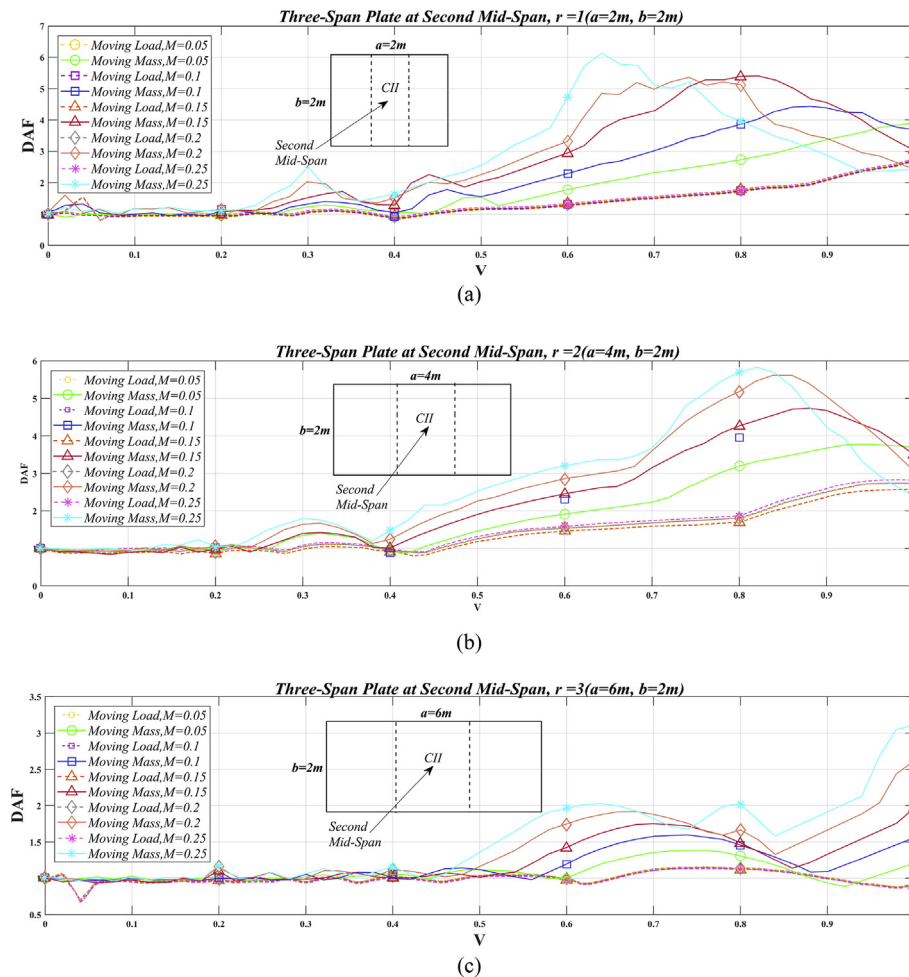
Fig. 23. The effect of moving mass velocity, **V**, on **DAF**, calculated at the second two-span plate's mid-span denoted by **CII**. Dashed lines are for moving load without inertia effect. (a) *r = 1*, (b) *r = 2* and (c) *r = 3*.

similar to the aforementioned procedure, so they are not repeated again. The main idea behind the factor β is to investigate the difference between responses under moving inertia mass and load. The values around unity for this factor may be interpreted as implying that the inertia effect has no significant influence on the **DAF** and the problem can be analyzed neglecting the inertia terms. On the other hand, when the factor takes on value greater than unity it means that the inertia terms would affect the response and must be highlighted in the calculations. By assessment of these three graphs, many useful results are obtained. At a glance at each graph with a specific aspect ratio, one can see that increasing the mass ratio would heighten the curves which means the difference between responses for both loading cases would no longer be negligible. On the other hand, surveying three graphs while the aspect ratio is enlarged, the maximum value for specified mass ratio, has a descending trend. For example, following the points on the curves for *M = 0.25* at the **V**= *0.8*, while we move from aspect ratio *1* to *3,* the corresponding values for β, takes values *1.3* down to *1.17* and *1.16*, respectively. It means that, by increasing the aspect ratio, the inertia property of moving mass has a less effect on the dynamic response of the plate.

3.3. Two-span plates

Fig. 13 shows a schematic of thin rectangular two-span plates under moving load excitation traveling on a rectilinear path with constant velocity.

In the plate, the spans are generated by a middle simply supported constraint and length of the plate is assumed to be free from support. Again we note that this boundary condition for two-span plate, SFSF, is similar to the single-span one. Also, **DAF** is calculated at the **CI** and **CII**

denoting the first and second mid-span points of the plate which are called *reference points*, respectively. Before analyzing the plate under moving load or mass, a free vibration analysis is carried out and the fundamental period of plate's vibration is derived and presented in Table 4. The results are reported based on using the BCOP method where *62* computational modes are considered into the analysis. Enlarging the aspect ratio would cause decrease of the natural frequency and lead to increase of the fundamental period of structure. This issue can be interpreted as decreasing trend of plate's stiffness.

3.3.1. The study on mass ratio parameter

The dynamic response of the plate at *reference points* for the first and second mid-span are studied here, while the mass ratio magnitude is varying and the aspect ratio of the plate is kept constant for each case.

Similar to the comments that were given in Sec. 3.2.1, here an analysis is performed for two-span plate with SFSF boundary condition, focusing on the effect of mass magnitude on the dynamic response of the plate. Figs. 14 and 15 show that by increasing the velocity of moving mass the difference between responses with and without inertia consideration is increased for both **CI** and **CII** *reference points*. By tracing the responses calculated at **CI** and **CII**, it is pointed out that in velocities below $\approx 0.2\ v'$, the mass inertia could be neglected from calculations and the problem could be solved in moving the load case. While the magnitude of velocity goes far from this value, the difference between a moving load and inertia mass is increased and the effect of inertia mass in calculations has to be accounted for. This issue would be located at the higher degree of importance when the mass weight is increased. On the other hand, the effect of aspect ratio can play a significant role in mitigating the difference between moving inertia mass and load. Therefore,
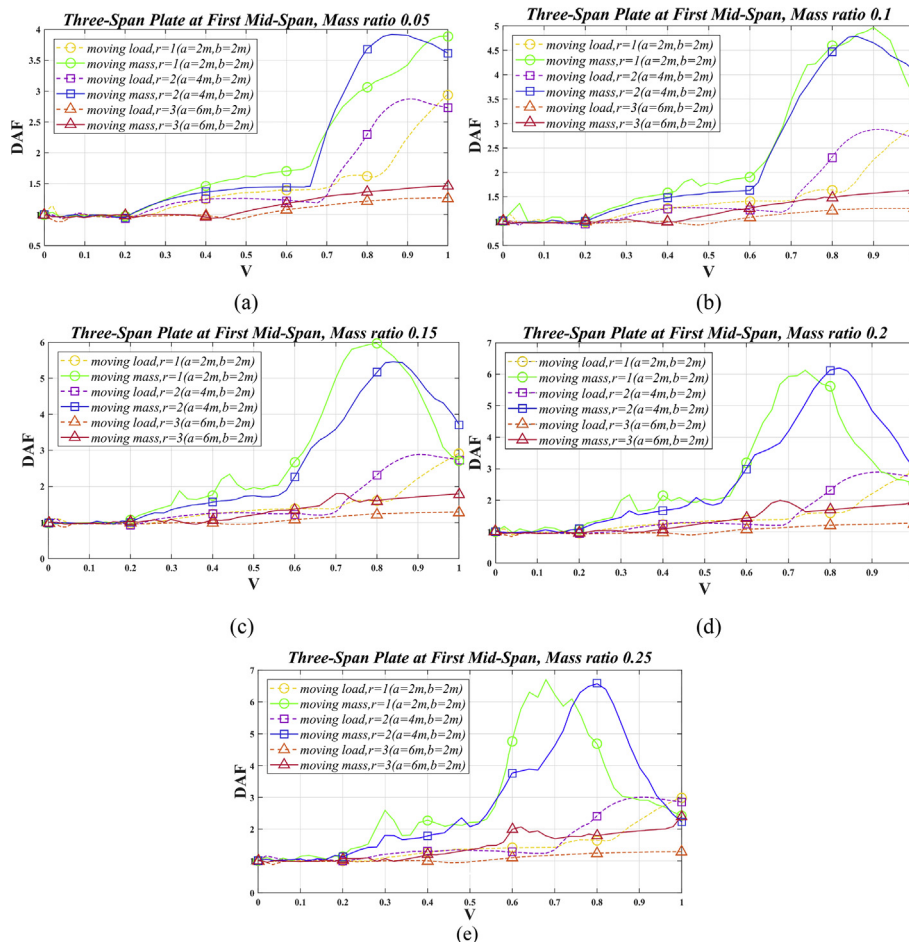
Fig. 24. Dynamic Amplification Factor, **DAF**, for the three-span SFSF plate, calculated at the first mid-span, **CI**, against non-dimensional velocity, **V**, under moving load and mass when the aspect ratio changes within values *1*, *2* and *3*. (a) *M = 0.05*, (b) *M = 0.1*, (c) *M = 0.15*, (d) *M = 0.2* and (e) *M = 0.25*.

by increasing the aspect ratio the aforementioned difference follows a decreasing trend.

3.3.2. The study on aspect ratio parameter

Completely similar to the parametric analysis performed before, here the aspect ratio effect on the plate's response under both cases of loading is investigated. The results are presented through several figures which contain graphs assigned for the constant value of mass weight. This time, the aspect ratio is put under assessment while the other parameters are taken to be constant. **DAF** for a two-span plate at both **CI** and **CII** points versus the velocity parameter, **V**, is studied with the aim of showing the effect of aspect ratio on the dynamic behavior of plate, with assumed boundary condition SFSF.

Figs. 16 and 17 reflect the fact that by increasing the aspect ratio of the plate in both *reference points*, the effect of inertia mass decreases and one can capture the solution in moving load conditions, improving accuracy and run time.

It would be useful if another parametric study is carried out here to evaluate the plate's response at two middle points of each span. Actually, the main idea behind this investigation is an assessment on the role of the location of the *reference point* of calculation. In other words, engineers and designers must have a prospective with the dynamic behavior of a multi-span plate, such that it could help them make an important decision in selecting the critical point of the structure under dynamic excitation and proceeding their design procedure based on it.

Here, a comprehensive parametric study has been carried out and the results have been presented through several graphs in Fig. 18. Within

these graphs, the main attention has been paid to the comparison between the results for **DAF** calculated at first and second plate's mid-span, while two other parameters of mass and aspect ratio has been kept constant.

An interesting result is obtained by tracing the manner of curves in Fig. 18. Generally, if the mass travels with velocities within ≈ 0.5 v′ to≈ 0.8 v′, the **DAF** for the second mid-span has a larger magnitude. Thus, it deserves to pay enough attention to it as a critical point in design. This trend is intensified when the aspect ratio of the plate is increased and in the plate with higher aspect ratios. As a general conclusion, the second mid-span point would have a larger **DAF.** Thus, it may be concluded that the design procedure must be carried out based on it.

3.3.3. Conversion factor

Similar to single-span plates and according to the aforementioned comments, here the conversion factor β is presented in Fig. 17 for both **CI** and **CII** points.

Fig. 19 shows that the most difference between responses for load and inertia mass at the first mid-span occurs at≈ 0.68 v′, and by increasing the aspect ratio of the plate this speed moves left to ≈ 0.62 v′. Therefore, this velocity approaches the lower value while the aspect ratio is increased. A different behavior is seen in Fig. 20 for the second *reference point*, **CII**, specifically at aspect ratio *1*, where the critical speed occurs in the velocity≈ 0.9 v′. This phenomenon can be interpreted by the fact that due to an almost high plate's stiffness, the maximum deflection is achieved at the higher velocity of moving mass. By increasing the aspect ratio we see a decreasing trend in the critical velocity which approaches≈ 0.47 v′,
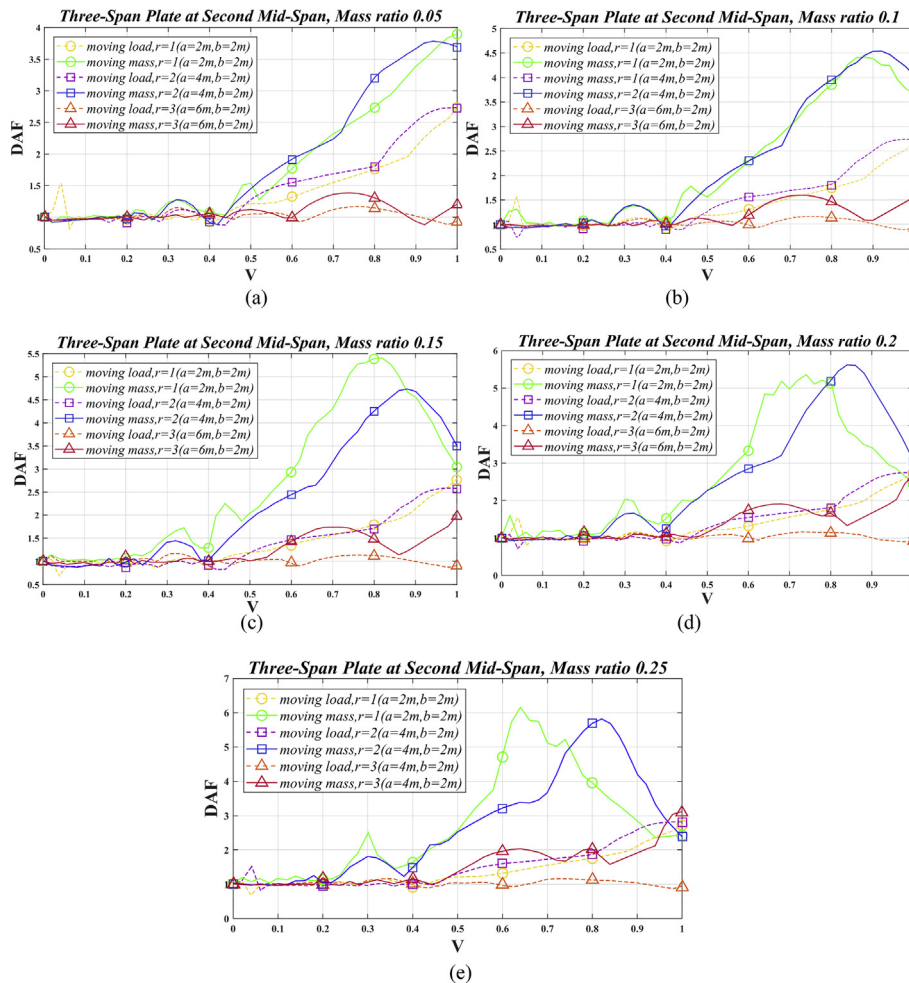
Fig. 25. Dynamic Amplification Factor, **DAF**, for the three-span SFSF plate, calculated at the second mid-span, **CII**, against non-dimensional velocity, **V**, under moving load and mass when the aspect ratio changes within values *1*, *2* and *3*. (a) *M = 0.05*, (b) *M = 0.1*, (c) *M = 0.15*, (d) *M = 0.2* and (e) *M = 0.25*.
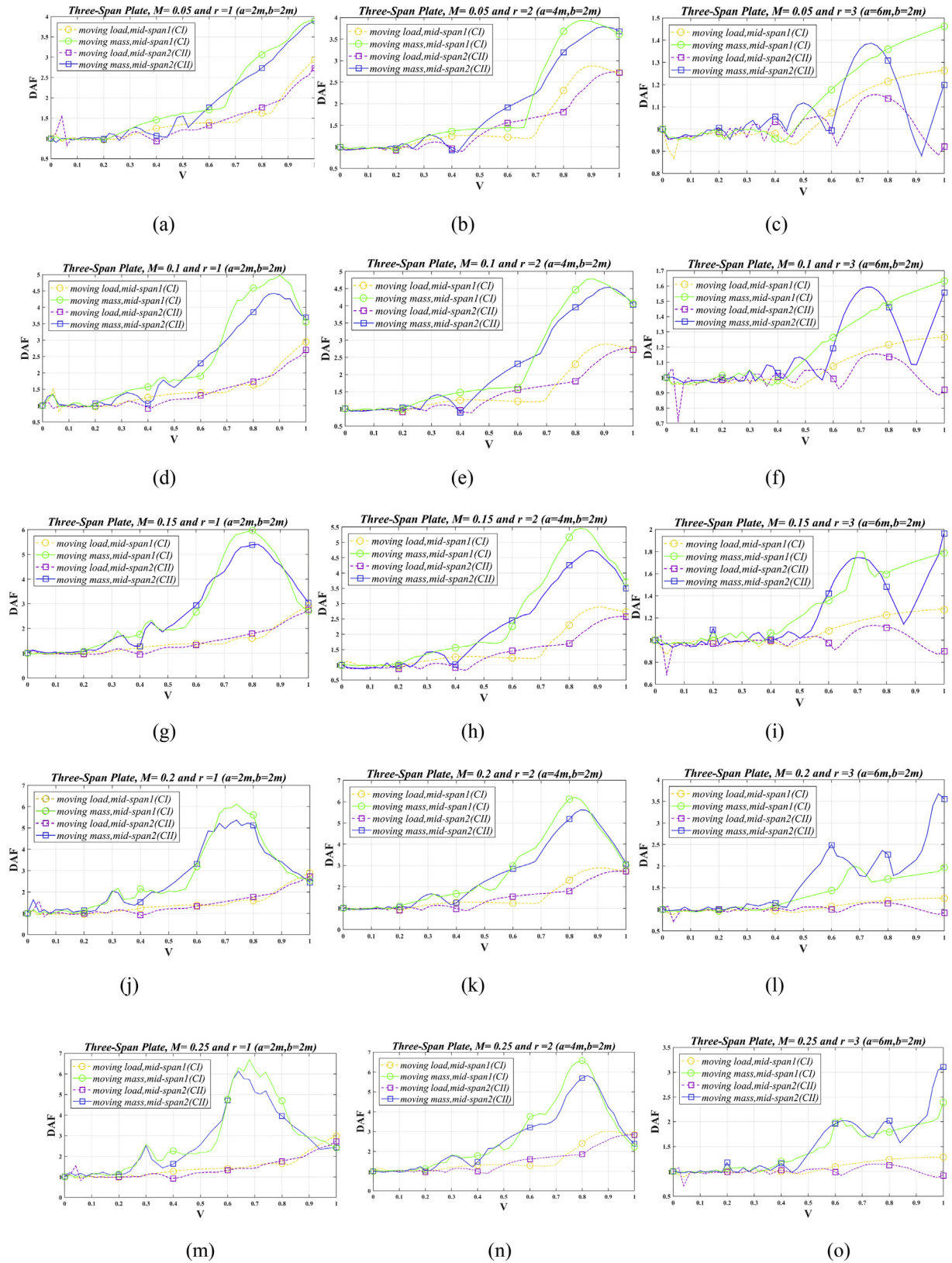
Fig. 26. The study on *reference point* (*CI* and *CII*) for a three-span plate. Each figure depicts **DAF** versus non-dimensional velocity, **V**, for constant mass and aspect ratio parameter. (a) *M = 0.05& r = 1,* (b) *M = 0.05 & r = 2,* (c) *M = 0.05 & r = 3,* (d) *M = 0.1 & r = 1,* (e) *M = 0.1 & r = 2,* (f) *M = 0.1 & r = 3,* (g) *M = 0.15 & r = 1,* (h) *M = 0.15 & r = 2,* (i) *M = 0.15 & r = 3,* (j) *M = 0.2 & r = 1* (k) *M = 0.2 & r = 2,* (l) *M = 0.2 & r = 3,* (m) *M = 0.25 & r =1,* (n) *M = 0.25 & r = 2,* (o) *M = 0.25 & r = 3.*

when the calculations are carried out at the second mid-span of the plate.

3.4. Three-span plates

In the last part of the paper and similar to the previous section, Fig. 21 shows a schematic for a three-span plate under moving mass excitation with constant velocity traveling on the rectilinear path. Using the same method and steps for two-span plates, numerical study is performed for three cases of aspect ratios and the results would be derived for the first and second mid-span, **CI** and **CII**, consequently. Finally, with the aim of showing the importance of inertia term contribution in the dynamic behavior of the plate, the conversion factor β is defined and presented in several graphs. One can easily find the critical velocity for such dynamic analysis and investigate its shifting, while some parameters are kept constant and the other is varying. Like two-span plates, the middle constraints is constructed by two simply supported staffs which divide the length of the plate into three parts with the same length. On two opposing edges, the plate would be assumed to be free from constraints. Again, we call this boundary condition, SFSF.

To derive the natural characteristics of plate's vibration, a free vibration analysis is run and similar to Sec 3.3, the fundamental period of three-span plate is reported in Table 5. Adding the middle constraints would lead to increased stiffness of three-span plates in comparison with two-span ones, at the same aspect ratio. According to Table 5, we can see the decreasing trend of natural frequency for a three-span plate by enlarging the aspect ratio (or increasing the trend of fundamental period of structure, conversely).

3.4.1. The study on mass ratio parameter

The influence of mass weight on the dynamic response of structure at first and second mid-span of a three-span plate is investigated here, which yields the spectrum of dynamic amplification factor versus non-dimensional velocity while the aspect ratio and the *reference point* are specified.

Adding middle constraints to the plate would cause an increased system stiffness, Thus, we can predict that we have vibrations with larger frequencies calculated at *reference point*. This behavior is seen in the first graphs of Figs. 22 and 23. Accordingly, the response of the plate for aspect ratio *1* at both **CI** and **CII** points were reported. In these Figures, specifically when the mass weight has increased, the curves could reach their peaks, so one can conclude that the critical speed must be considered within $\approx 0.6\,v'$ up to $\approx 0.8\,v'$. By increasing the aspect ratio of the plate, the curves in Figs. 21 and 22 become more smooth such than both the maximum **DAF** accompanied with decreased critical velocity. It can be seen that in Figs. 22 and 23, for aspect ratios *1* and *2* in velocities below$\approx 0.2\,v'$. The problem could be solved without considering the inertia effect of a moving mass, preserving the acceptable accuracy. For aspect ratio *3*, this velocity has increased to$\approx 0.4\,v'$. This behavior explains the fact that by decreasing the stiffness of the plate, the role of the inertia of the mass moving on a three-span plate has decreased. Hence, the solution of equations of motion in moving load would be adopted.

3.4.2. The study on aspect ratio parameter

The role of aspect ratio on the response of the plate is very important as shown in the previous section. For that reason, the effect of aspect ratio
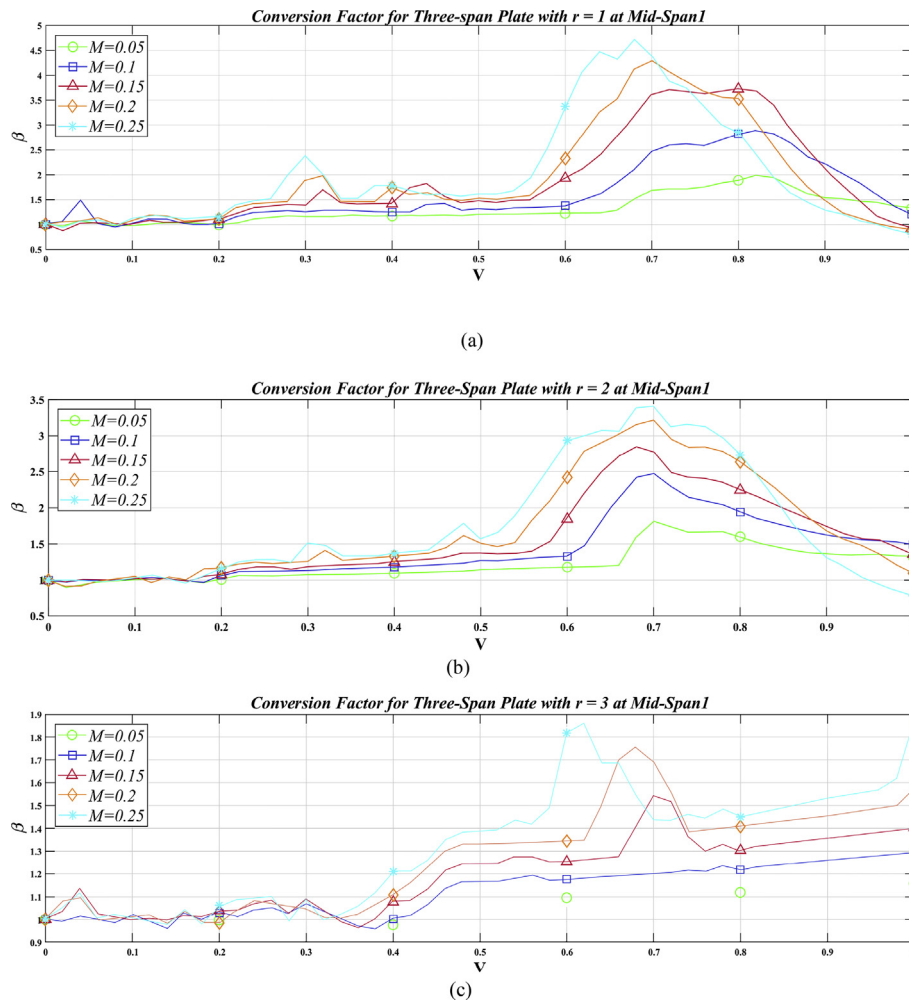
Fig. 27. Conversion factor for a three-span plate with SFSF boundary condition versus non-dimensional velocity calculated at the first mid-span **CI** with specified mass and aspect ratio. (a) *r = 1*, (b) *r = 2* and (c) *r = 3*.

Conversion Factor for Three-Span Plate with r = 1 at Mid-Span2

(a)

Conversion Factor for Three-Span Plate with r = 2 at Mid-Span2

(b)

Conversion Factor for Three-Span Plate with r = 3 at Mid-Span2

(c)
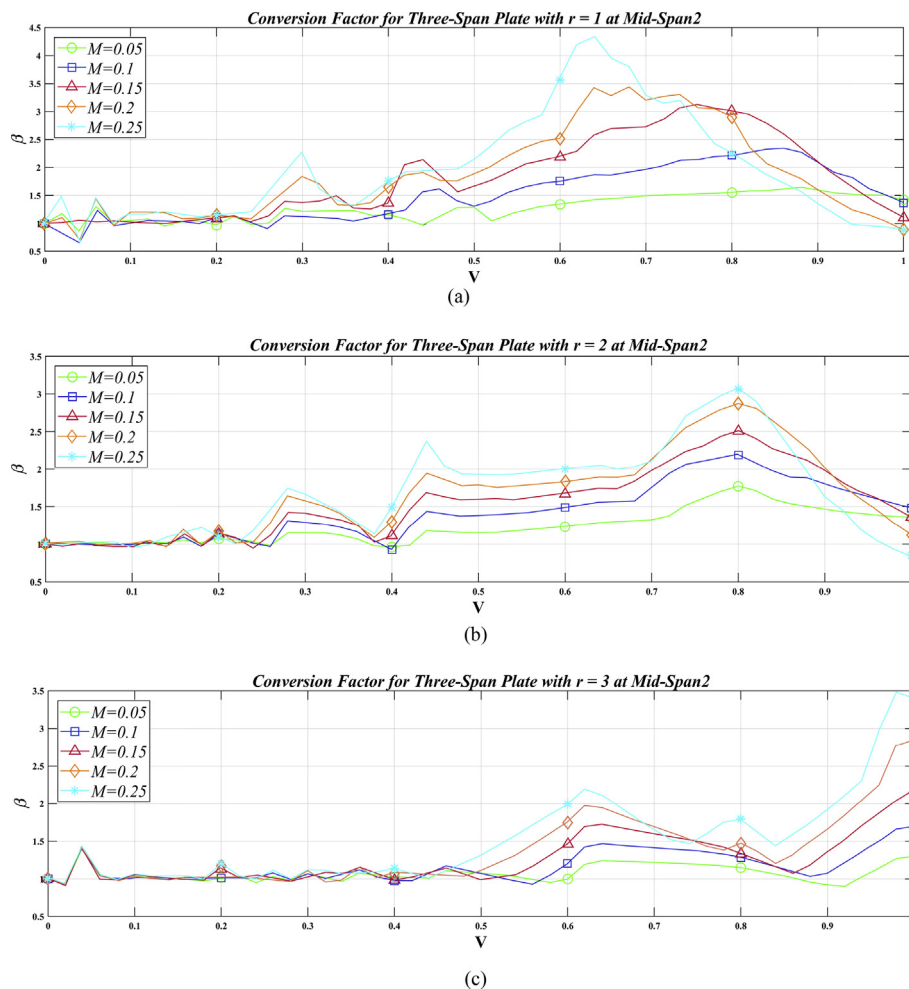
Fig. 28. Conversion factor for three-span plates with SFSF boundary conditions versus non-dimensional velocity calculated at the second mid-span **CII** with specified mass and aspect ratio. (a) *r = 1*, (b) *r = 2* and (c) *r = 3*.

is investigated exclusively in this section. The **DAF** of mid-span points versus non-dimensional velocity with constant mass ratio is shown in Figs. 24 and 25.

Investigating on the aspect ratio effect of the plate's **DAF** shows that increasing of this parameter could mitigate the **DAF** of plate's central point remarkably.

Similar to the procedure that was carried out for a two-span plate, the investigations could be performed for two *reference points* **CI** and **CII**. Therefore, the response of the plate's central point for both **CI** and **CII** are depicted into the same graphs versus non-dimensional velocity. In each Figure the mass and aspect ratio are assumed to be constant and the curves show both loading cases, including and ignoring the inertia effects.

Fig. 26 shows the five series of graphs including the effects of first and second mid span points of a three-span plate it is acted upon by a moving load and mass, where the magnitude of mass and aspect ratio are considered to be constant. Clearly, these Figures reflect that almost in all velocity parameters the **DAF** of the first mid span has a greater value than that of the second one. However, this trend has become quiet by increasing the aspect ratio, while mass ratio is considered to be constant.

3.4.3. Conversion factor

The conversion factor for a three-span plate is presented in Figs. 27 and 28, from which one can derive the velocity at which there is the most difference between the load and inertia mass cases. Therefore, the fact is noted that in such velocities the analysis has to be carried out considering the formulation when the inertia terms are accounted for.

When the values of β have a small deviation from unity, one may conclude that the problem can be solved without mass inertia effects. Thus, it would be acceptable to assume that the load moving on the plate's surface is a concentrated force. This margin is extended when the aspect ratio is increased. However, as a general conclusion for the first mid-span *reference point* it could be said that most deviation from unity is occurred within ≈ 0.6 *v'* up to ≈ 0.8 *v'*. In addition, the factor would be strictly affected when the mass weight moving on the plate is increased For instance, if we follow the curve pertaining to three-span plate with aspect ratio *2* pertaining to the second mid-span, it could be interpreted that the maximum value of the corrective factor increases while the magnitude of mass ratio parameter is increased, within the values of *1.7* up to *3.2*. This behavior shown in the curves could point out the fact that by increasing the mass, the difference between the plate's response under moving load and inertia mass cannot be ignored and the problem must be solved with full terms of mass inertia. On the other hand, the peaks occur at ≈ 0.8 *v'* which indicates the critical velocity for this case.

4. Conclusion

In this study, a thin rectangular multi-span plate under moving concentrated inertia mass excitation traveling on an arbitrary path is considered. The spans generated by the middle constraints comply with simply supported conditions. The partial differential equations of motion were derived and solved by the Galerkin method in a general form where the mode shapes were generated by the Boundary Characteristic Orthogonal Polynomials (BCOP) as spatial functions. The powerful

method of Matrix Exponential was employed to solve the problem in the time domain. The plate with single, two and three spans with simply supported constraints at width and free condition along the length were investigated. The results were presented within numerous Figures of Dynamic Amplification Factor, **DAF**, versus non-dimensional velocity, **V**, of moving mass.

As a joint result, for single, two and three-span plates the investigation showed that increasing the magnitude of the mass ratio, traveling on the plate, **DAF** of plate's mid-span remarkably increases. Moreover, the difference between a plate's response in both cases of moving load and mass have increased so the inertia effects of moving mass have to be considered. The increasing trend of aspect ratio could mitigate the **DAF** of plate specifically in high velocities of moving loads.

About two-span plates, the following conclusions can be drawn. Generally the first mid-span shows a more critical behavior under moving mass excitation, except for the velocity parameter between *0.4* and *0.6*, where the second mid-span must be consider crucial. This manner is intensified when the aspect ratio of the plate is increased. Decreasing the aspect ratio, the responses of two *reference points* much closer to each other. In addition, the critical velocity is decreased while the aspect ratio is increased. For all cases, the magnitude of the mass would cause more deflection and it magnifies the dynamic effect of moving mass.

Similarly for thee-span plates, increasing the mass magnitude results in increased dynamic deflection and the critical velocity is mitigated. That is, the plate undergoes a more critical condition. Clearly, the inertia effect is mitigated when the length of the plate is increased and actually the first mid-span plays a more critical role than the second one. The critical velocity of the second mid span as a *reference point*, has a higher value and it means that it could be reached to a maximum deflection later than the first mid span.

As a general achievement, adding the constraint to the plate and changing the plate from one to two and then to three spans increases the plate stiffness and yields to more deflection. In the same case, the first mid span of three-span plates shows a more important behavior under moving inertia load. In addition, the critical velocity for three-span plates is higher than that of the two-span ones keeping the other parameters constant.

This means that given a fixed length while adding spans to the plate would result in higher plate deflection of the plate supporting a moving mass with higher speeds.

Declarations

Author contribution statement

Hooman Kashani Rad: Conceived and designed the experiments; Performed the experiments; Analyzed and interpreted the data; Wrote the paper.

Mansour Ghalehnovi: Conceived and designed the experiments; Contributed reagents, materials, analysis tools or data.

Hashem Shariatmadar: Contributed reagents, materials, analysis tools or data.

Funding statement

Competing interest statement

The authors declare no conflict of interest.

Additional information

No additional information is available for this paper.

References

[1] L. Fryba, Vibration of Solids and Structures under Moving Loads, Thomas Telford, London, 1999.

[2] H. Ouyang, Moving load dynamics problem: a tutorial (with a brief overview), Mech. Syst. Signal Process. 25 (6) (2011) 2039–2060.

[3] J.E. Akin, M. Mofid, Numerical solution for response of beams with moving mass, ASCE J. Struct. Eng. 115 (1) (1989) 120–131.

[4] E. Esmailzadeh, M. Ghorashi, Vibration analysis of beams traversed by uniform partially distributed moving masses, J. Sound Vib. 184 (1995) 9–17.

[5] H.P. Lee, The dynamic response of a Timoshenko beam subjected to a moving mass, J. Sound Vib. 198 (1996) 249–256.

[6] A. Yavari, M. Nouri, M. Mofid, Discrete element analysis of dynamic response of Timoshenko beams under moving mass, Adv. Eng. Software 33 (2002) 143–153.

[7] A. Nikkhoo, F.R. Rofooei, M.R. Shadnam, Dynamic behavior and modal control of beams under movingmass, J. Sound Vib. 306 (2007) 712–724.

[8] C. Bilello, L.A. Bergman, D. Kuchma, Experimental investigation of a small-scale bridge model under a moving mass, ASCE J. Struct. Eng. 130 (2004) 799–804.

[9] C. Bilello, L.A. Bergman, Vibration of damaged beams under a moving mass: theory and experimental validation, J. Sound Vib. 274 (2004) 567–582.

[10] G.V. Rao, Linear dynamics of an elastic beam under moving loads, ASME J. Vib. Acoust. 122 (2000) 281–289.

[11] J.S. Wu, C.W. Dai, Dynamic responses of multispan nonuniform beam due to moving loads, ASCE J. Struct. Eng. 113 (3) (1987) 458–474.

[12] H.P. Lee, Dynamic response of a beam with intermediate point constraints subjected to a moving load, J. Sound Vib. 171 (3) (1994) 361–368.

[13] P.K. Chaterjee, T.K. Datta, C.S. Surana, Vibration of continuous bridges under moving vehicles, J. Sound Vib. 169 (2) (1994) 619–632.

[14] M. Ichikawa, Y. Miyakawa, A. Matsuda, Vibration analysis of the continuous beam subjected to a moving mass, J. Sound Vib. 230 (3) (2000) 493–506.

[15] K. Kiani, A. Nikkhoo, B. Mehri, Assesing dynamic response of multi span viscoelastic thin beam under a moving mass via generalized moving least square method, J. Achta. Mech. (2010).

[16] O. Civalek, Free vibration of carbon nanotubes reinforced (CNTR) and functionally graded shells and plates based on FSDT via discrete singular convolution method, Composites Part B 50 (2013) 171–179.

[17] O. Civalek, Nonlinear dynamic response of laminated plates resting on nonlinear elastic foundations by the discrete singular convolution-differential quadrature coupled approaches, Composites Part B 50 (2013) 171–179.

[18] A. Cifuentes, S. Lalapet, A general method to determine the dynamic response of a plate to a moving mass, Comput. Struct. 42 (1992) 31–36.

[19] J.A. Gbadeyan, S.T. Oni, Dynamic behavior of beams and rectangular plates under moving loads, J. Sound Vib. 182 (1995) 677–695.

[20] M.R. Shadnam, M. Mofid, J.E. Akin, On the dynamic response of rectangular plate, with moving mass, Thin-Walled Struct. 39 (2001) 797–806.

[21] A. Nikkhoo, F.R. Rofooei, Parametric study of the dynamic response thin rectangular plates traversed by a moving mass, J. Achta. Mech. (2011).

[22] H. Takatabake, Dynamic analysis of rectangular plates with stepped thickness subjected to moving loads including additional mass, J. Sound Vib. 213 (5) (1998) 829–842.

[23] M.H. Huang, D.P. Thambiratnam, Deflection response of plate on Winkler foundation to moving accelerated loads, Eng. Struct. (2001) 1134–1141.

[24] T. Ghazvini, A. Nikkhoo, H. Allahyari, M. Zapulli, Dynamic response analysis of thin rectangular plate of varying thickness to traveling inertia loads, J. Braz. Soc. Mech. Sci. Eng. 38 (2) (2015) 403–411.

[25] A. Nikkhoo, M.E. Hassanabadi, J.V. Amiri, Vibration of thin rectangular plate subjected to series of inertial loads, Mech. Res. Commun. 55 (2014) 105–113.

[26] J.A. Gbadyan, M.S. Dada, Dynamic response of a Mindlin elastic rectangular plate under a distributed moving mass, Int. J. Mech. Sci. 48 (2006) 323–340.

[27] J.V. Amiri, A. Nikkhoo, M.R. Davood, M.E. Hassanabadi, Vibration analysis of Mindlin elastic plate under moving mass excitation y eigenfunction expansion method, Thin-Walled Struct. 62 (2013) 53–54.

[28] S.A. Eftekhari, A.A. Jafari, Vibration of an initially stressed rectangular plate due to an accelerated traveling mass, Sci. Iran. 19 (5) (2012) 1195–1213.

[29] J.J. Wu, Vibration of rectangular plate undergoing force moving along a circular path, Finite Elem. Anal. Des. 40 (2003) 41–60.

[30] J.J. Wu, Vibration analysis of inclined flat plate subjected to moving loads, J. Sound Vib. 299 (2007) 373–387.

[31] J.J. Wu, Use of moving distributed mass element for the dynamic analysis of a flat plate undergoing a distributed load, Int. J. Numer. Methods Eng. 71 (2007), 374-62.

[32] I. Essen, A new finite element for transverse vibration of rectangular thin plates under a moving mass, Finite Elem. Anal. Des. 66 (2013) 26–35.

[33] S. Qinghua, S. Jiahao, L. Zhanqiang, Dynamic analysis of thin rectangular plates of arbitrary boundary conditions under moving loads, Int. J. Mech. Sci. 002 (2016) 0–4703.

[34] A.W. Leissa, Vibration of Plates, US Government Printing Office, Washington, DC, 1969.

[35] S. Chakraverty, Vibration of Plates, CRC Press, Taylor & Francis Group, New York, 2009.

[36] W.L. Brogan, Modern Control Theory, Prentice-Hall, New Jersey, 1991.